

# Quantum-state mapping between multilevel atoms and cavity light fields

A.S. Parkins

*Universität Konstanz, Fakultät für Physik, D-78434 Konstanz, Germany*

P. Marte and P. Zoller

*Joint Institute for Laboratory Astrophysics and Department of Physics, University of Colorado, Boulder, Colorado 80309-440*

O. Carnal and H.J. Kimble

*Norman Bridge Laboratory of Physics 12-33, California Institute of Technology, Pasadena, California 91125*

(Received 20 April 1994)

A scheme for the preparation of Fock states and general superposition states of the electromagnetic field in a cavity is studied in detail. The scheme uses adiabatic passage in a strongly coupled atom-cavity system to “map” atomic ground-state Zeeman coherence onto the cavity-mode field. We model photon-counting and homodyne measurements of the field exiting the cavity and demonstrate the possibility of generating and detecting highly nonclassical states of the field with parameter values close to currently realizable experimental values. The adiabatic passage process is also reversible, enabling cavity-mode fields to be mapped onto atomic ground-state Zeeman coherence. Application of this property to the measurement of cavity fields is discussed, with particular consideration given to a possible scheme for quantum measurement of the intracavity photon number.

PACS number(s): 42.50.Dv, 42.50.Lc

## I. INTRODUCTION

Nonclassical electromagnetic fields exhibit statistical properties that cannot be associated with any classical stochastic process. That is, nonclassical electromagnetic fields require an explicitly quantum-mechanical description. Spectacular recent advances in quantum optics have led to the experimental realization of such fields. Quadrature-squeezed and sub-Poissonian light fields are two prominent examples [1–3]. Quadrature-squeezed light exhibits reduced quantum fluctuations, below the vacuum-state level, in one quadrature phase amplitude of the field. Sub-Poissonian, or intensity-squeezed, light is characterized by an intensity distribution narrower than a Poissonian distribution, which corresponds to a reduction in intensity fluctuations below the level of a coherent light field.

Interest in these nonclassical light fields arises from the potential applications such fields may have in optical systems. In particular, the reduced fluctuations exhibited by these states of light offer the possibility of enhanced measurement sensitivity beyond the standard quantum limit set by vacuum fluctuations. Theoretical studies also indicate that fundamental atomic processes should be altered through interaction with nonclassical light [4].

A particularly interesting and topical avenue of research into the generation of nonclassical light fields is that associated with cavity quantum electrodynamics, in which beams of atoms interact strongly with a single quantized field mode of a cavity [5]. In both the microwave [6,7] and optical [8,9] regimes it is now possible to realize situations in which the single-atom-cavity-mode coupling strength exceeds spontaneous emission and cavity loss rates, so that coherent evolution of the coupled

system predominates, or at least produces observable effects. In microwave experiments this is achieved by using Rydberg atoms and very high- $Q$  superconducting cavities, so that spontaneous emission and cavity damping are quite negligible on the time scale of the atom-field interaction. Properties of the cavity field are inferred from interrogation of atoms exiting the cavity. In optical experiments spontaneous emission is significant, but the strong-coupling regime can be reached via high-finesse cavities and very small cavity-mode volumes. In contrast to the microwave regime, one has direct access to the optical field in the form of light transmitted through the cavity mirrors and hence one can employ a number of direct measurement schemes such as photon counting and homodyne detection.

The predominance of coherent evolution in these configurations makes cavity quantum electrodynamics a favorable candidate for the realization of uniquely quantum-mechanical states of light. Relevant examples are Fock (or number) states, which have no intensity fluctuations (corresponding to the “ultimate” sub-Poissonian field), and coherent superposition states, which, in the case that the superposed states can be regarded as macroscopically, or classically, distinguishable, are referred to as “Schrödinger cat” states.

A variety of theoretical proposals have been put forward for the generation of such states [10–19]. Brune *et al.* [11,14], have shown that repeated measurements of the dispersive phase shift experienced by Rydberg atoms traversing a microwave cavity produce a collapse of the cavity-field photon distribution into a pure photon-number state. A variation of this scheme involving an initial coherent state and single-atom interaction and detection can generate a Schrödinger-cat state of the field [14,16]. Measurements of the dipole-force-induced deflec-

tion of an atomic beam from the standing-wave cavity mode may also in principle yield Fock states, as shown by Holland *et al.* [12], while Cirac *et al.* [13] have demonstrated a scheme in which Fock states can be generated via the observation of quantum jumps to a metastable atomic level. The technique of Slosser *et al.* [15] for the generation of coherent superposition states assumes a sequence of polarized two-level atoms passing through a microwave cavity and invokes the concept of “trapping states” in a micromaser [5]. In a similar vein, Vogel *et al.* [17] have recently demonstrated theoretically that a sequence of suitably prepared two-level atoms can drive a cavity mode into an arbitrary superposition state, provided that each atom is measured to be in a particular state following its interaction with the field. A scheme based upon the same mechanism, but employing two-photon interactions in a micromaser, has also been described by Garraway *et al.* [18]. Finally, a scheme based on the adiabatic transformation of system eigenstates involving continuous tuning of the cavity frequency was proposed by Raimond *et al.* [10] as a means of producing Fock states. In all of the above-mentioned schemes, the effects of atomic spontaneous emission are avoided through the use of either slowly decaying atomic levels (e.g., Rydberg atoms) or far-off-resonance (and hence weak) atom-field interactions.

The purpose of the present paper is to examine in detail a scheme put forward recently by us for the preparation of Fock states and coherent superposition states in a cavity [19]. As with the proposal of Raimond *et al.* [10], our scheme is based upon the adiabatic transformation of an eigenstate of the atom-cavity system. The feature of the scheme that sets it apart from previous work, however, and which gives it particular appeal, is that the relevant adiabatically evolving eigenstate contains no contribution from excited atomic states, even under the condition of resonant atom-field interaction. Hence atomic spontaneous emission, in principle, plays no role in the system dynamics, irrespective of the spectral regime we may be considering and of atom-field detuning. The possibility of experiments in the optical regime, especially with regard to the generation of superposition states, makes this scheme of particular interest, we believe, and indeed the emphasis of the work to be presented here is upon configurations appropriate to optical experiments.

In practical terms, our scheme requires the passage of an atom (or atoms) with Zeeman substructure through overlapping cavity and laser fields. The adiabatic passage technique allows for coherent superpositions of atomic ground-state Zeeman sublevels to be “mapped” directly onto coherent superpositions of cavity-mode number states. This ability arises from the independent evolution of different “families” of states of the coupled atom-cavity system. Hence the generality of the superpositions that can be produced in the cavity is limited only by the extent to which one can prepare general superpositions of atomic ground-state Zeeman sublevels (for example, using optical or radio-frequency pumping) and, of course, by the number of available Zeeman sublevels (i.e., by the angular momentum quantum number of the atomic level). Another significant feature of the scheme

is that following the transfer the atomic population is in a *single* atomic state, thereby avoiding the introduction of atomic-state “measurement noise.”

The outline of this paper is as follows. In Sec. II we describe the mechanism of adiabatic passage in an atom-cavity-mode system and give the conditions necessary for such a scheme to operate efficiently. In Sec. III we present numerical results for the situation in which adiabatic passage produces a coherent shift of the cavity-mode photon distribution. Of most interest to us here is the case in which the cavity field is initially in the vacuum state and passage of an atom through the interaction region yields a Fock state of the field. As mentioned above, we put emphasis upon the optical regime, primarily restricting ourselves to values of coupling strengths, cavity damping, and spontaneous emission damping that are of relevance to existing experiments and to configurations that should be viable with realistic improvements. Also in this vein, we model photon-counting measurements on the field transmitted through the cavity mirrors, taking into account finite detector efficiencies so that we may gauge the practicality of detecting Fock states of the field generated by this scheme. In Sec. IV we describe the mechanism by which coherent superposition states may be generated and present numerical results in certain regimes and for various possible forms of superposition states. With an eye towards possible experiments, we consider balanced homodyne measurements of the cavity field as a means of detecting these states. Sections V and VI are devoted to discussions of possible further applications of the adiabatic passage scheme. More specifically, in Sec. V we describe a variation on the adiabatic passage scheme whereby coherent superpositions of fields in macroscopically separated cavities may be produced, while in Sec. VI we discuss the potential of adiabatic passage for the measurement of cavity fields, with particular emphasis on the possibility of quantum measurement of the intracavity photon number. Finally, in the Conclusion we touch briefly upon some experimental considerations.

## II. ADIABATIC PASSAGE IN AN ATOM-CAVITY SYSTEM

Given that a system is described by a time-varying Hamiltonian  $H(t)$ , the adiabatic theorem applied to this system for the interval of time from  $t_0$  to  $t_1$  can be stated in its simplest form as follows [20]: If the evolution from time  $t_0$  to time  $t_1$  is sufficiently slow, then if the system is initially in an eigenstate of  $H(t_0)$  it will pass into the eigenstate of  $H(t_1)$  that derives from it by continuity.

Making use of this property of adiabatically evolving quantum systems, Raimond *et al.* [10] proposed a scheme for the preparation of Fock states in which initially excited Rydberg atoms pass through a microwave cavity, the resonant frequency of which is continuously varied during the atomic transit time. With an appropriate time dependence of the atom-cavity detuning, the initial eigenstate describing the atom-cavity system adiabatically evolves into a final eigenstate corresponding to the

atoms being in the ground state and to the cavity mode being in a Fock state. Although the evolving eigenstate contains a contribution from the excited atomic state, nonadiabatic transitions induced by spontaneous emission do not represent a significant problem as long as one remains in the microwave regime.

The adiabatic passage scheme that we are concerned with has its origins in studies of coherent population transfer between atomic ground-state levels [21–24] and more recently in work on coherent atomic-beam deflection [25]. These studies demonstrated that the adiabatic evolution of a certain atomic eigenstate, given the presence of appropriately ordered time-dependent laser pulses, could facilitate the coherent and complete transfer of atomic population to a single ground state. The remarkable feature of this eigenstate, which enables atomic coherence to be preserved, is that it has no contribution from excited atomic states. That is, under suitable operating conditions, excited atomic states are never populated during the evolution and spontaneous emission does not figure in the dynamics of the system.

The adiabatic transfer between atomic ground states can also be interpreted in terms of Raman transitions induced by a pair of laser fields. These transitions involve the exchange of precise numbers of photons between the two laser fields, with a similarly precise number of momentum “kicks” given to the atom in the directions of the laser beams. In the case that the laser beams are counterpropagating, it follows that an atom can experience a substantial and controlled deflection in one direction. The potential of this characteristic feature for use in atomic interferometry has been pointed out recently [25].

### A. Basic description: Three-level $\Lambda$ atom

The theoretical analysis of coherent population transfer in atomic systems via adiabatic passage has been given in detail in Refs. [21–24]. A clear and simple description of the method is best given for the elementary case of a three-level  $\Lambda$  atom subject to two incident light fields. Our analysis of this system is completely analogous to the earlier work on coherent population transfer. However, previous work was not concerned with the statistics of the light fields, which were typically coherent laser fields and were thus treated as classical fields. In contrast, we now consider one of the light fields to be the field mode of a cavity. In terms of our theoretical model, this necessitates the quantization of one of the fields coupled to the atom. The properties and statistics of this quantized field mode are the focus of our attention in this paper.

#### 1. Dark state

We consider a single three-level atom with two ground states  $|g_1\rangle$  and  $|g_2\rangle$  (for simplicity we consider these states to have the same energy) coupled to an excited state  $|e\rangle$  via, respectively, a classical laser field  $\Omega(t)$  of frequency

$\omega_L$  and a cavity-mode field of frequency  $\omega$ . For the moment, we neglect atomic spontaneous emission and cavity damping, but these will be added to the model when we carry out numerical calculations in the ensuing sections. The Hamiltonian for this system can thus be written as

$$H(t) = \hbar\omega a^\dagger a + \hbar\omega_{eg}|e\rangle\langle e| - i\hbar g(t)(|e\rangle\langle g_2|a - \text{H.c.}) + i\hbar\Omega(t)(|e\rangle\langle g_1|e^{-i\omega_L t} - \text{H.c.}), \quad (1)$$

where  $a$  is the annihilation operator for the cavity mode and  $g(t)$  gives the atom–cavity-mode coupling strength. The time dependence of  $\Omega(t)$  and  $g(t)$  is provided simply by the motion of the atom across the laser- and cavity-field profiles.

The Hamiltonian  $H(t)$  has the property that it couples only states within the family, or manifold,  $\{|g_1, n\rangle, |e, n\rangle, |g_2, n+1\rangle\}$ , where  $|g, n\rangle \equiv |g\rangle \otimes |n\rangle$ ,  $|e, n\rangle \equiv |e\rangle \otimes |n\rangle$ , and  $|n\rangle$  represents an  $n$ -photon Fock state of the cavity mode. Such a family is depicted in Fig. 1(a). In a frame rotating at the frequency  $\omega$ , the adiabatic energy eigenvalues of the Hamiltonian associated with a particular family of states take the forms

$$E_n = n\hbar\omega, \\ E_n^\pm = n\hbar\omega + \frac{1}{2}\hbar\{\Delta \pm [\Delta^2 + 4g(t)^2(n+1) + 4\Omega(t)^2]^{1/2}\},$$

where we have assumed that  $\omega = \omega_L$  and  $\Delta = \omega_{eg} - \omega$  is the detuning. Of particular interest to us is the eigenstate corresponding to  $E_n = n\hbar\omega$ , which is given by

$$|E_n\rangle = \frac{g(t)\sqrt{n+1}|g_1, n\rangle + \Omega(t)|g_2, n+1\rangle}{\sqrt{\Omega(t)^2 + g(t)^2(n+1)}}. \quad (2)$$

This eigenstate does not contain any contribution from the excited state (hence the term “dark state”) and is independent of the detuning  $\Delta$ . For completeness, the eigenstates  $|E_n^\pm\rangle$  are

$$|E_n^\pm\rangle = \mathcal{N}_\pm(t)^{-1/2}\{i\Omega(t)|g_1, n\rangle + \lambda_\pm(t)|e, n\rangle - ig(t)\sqrt{n+1}|g_2, n+1\rangle\}, \quad (3)$$

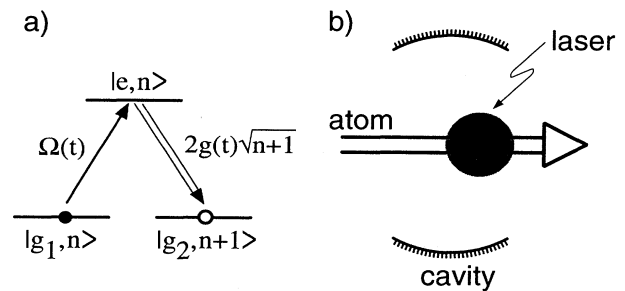


FIG. 1. (a)  $\Lambda$  three-level atom. (b) Proposed configuration for the preparation of Fock states using three-level atoms. The propagation direction of the pump laser is perpendicular to the page.

where  $\mathcal{N}_\pm(t) = g(t)^2(n+1) + \lambda_\pm(t)^2 + \Omega(t)^2$  and

$$\lambda_\pm(t) = \frac{1}{2} \left\{ \Delta \pm [\Delta^2 + 4g(t)^2(n+1) + 4\Omega(t)^2]^{1/2} \right\}. \quad (4)$$

## 2. Time evolution

The state  $|E_n\rangle$  exhibits the following asymptotic behavior as a function of time:

$$|E_n\rangle \rightarrow \begin{cases} |g_1, n\rangle & \text{for } \Omega(t)/g(t) \rightarrow 0 \\ |g_2, n+1\rangle & \text{for } g(t)/\Omega(t) \rightarrow 0. \end{cases} \quad (5)$$

Given that the time evolution of the system is adiabatic, Eq. (5) demonstrates the possibility for the adiabatic transformation of the state  $|g_1, n\rangle$  into the state  $|g_2, n+1\rangle$

(and vice versa). For example, if, as the atom enters the interaction region, the state of the atom-cavity system is given by  $|g_1, n\rangle$ , then, for the pulse sequence (as “seen” by the atom traversing the cavity and laser fields) in which  $\Omega(t)$  is time delayed with respect to  $g(t)$ , the final state of the system as the atom exits the interaction region will be  $|g_2, n+1\rangle$ . Such a pulse sequence would be realized in the experimental configuration depicted in Fig. 1(b).

## 3. Shift of the photon distribution

Given the evolution described above, it follows that the passage of an atom through the cavity and laser fields produces a single-photon “shift” of the cavity-mode photon distribution. This is summarized by the transformation equation for the density operator of the atom-cavity system:

$$\rho \equiv |g_1\rangle\langle g_1| \otimes \rho_F \equiv |g_1\rangle\langle g_1| \otimes \sum_{n,m} |n\rangle\langle m| \langle m|\rho_F|n\rangle \longrightarrow |g_2\rangle\langle g_2| \otimes \sum_{n,m} |n+1\rangle\langle m+1| \langle m|\rho_F|n\rangle \equiv \rho'. \quad (6)$$

That is, an atom prepared in the state  $|g_1\rangle$  leaves the cavity in state  $|g_2\rangle$  with probability one and the cavity-mode density operator following the passage is given simply by

$$\rho'_F = \text{Tr}_A(\rho') = \sum_{n,m} |n+1\rangle\langle m+1| \langle m|\rho_F|n\rangle, \quad (7)$$

where  $\text{Tr}_A(\cdot)$  denotes the trace over the atom. The photon distribution is shifted by exactly one photon. [Note that the forms of the coupling terms in the Hamiltonian (1) are such that phase shifts occurring during the adiabatic transformation are identically zero.] Obviously, the transit of  $N$  such atoms shifts the distribution by exactly  $N$  photons. For the case of an initial vacuum state of the cavity mode,  $\rho_F = |0\rangle\langle 0|$ , this corresponds to the generation of an  $N$ -photon Fock state  $\rho'_F = |N\rangle\langle N|$ , provided, of course, that cavity losses are negligible during the interval between the first and last atoms.

### B. Atomic $J_g = N \rightarrow J_e = N - 1$ transition: Multiple-photon shift

One need not restrict oneself to single-photon shifts per atom. The same analysis described above can be applied to more complicated atomic-level configurations, with the most obvious generalization being to an atom possessing Zeeman substructure. In particular, we shall concentrate on a  $J_g = N \rightarrow J_e = N - 1$  atomic transition, where  $J_g$  and  $J_e$  denote, respectively, the total angular momentum quantum numbers of the ground and excited atomic levels. The laser field is assumed to be  $\sigma^+$  polarized and the cavity field  $\pi$  polarized: in this way the photon shift per atom is maximized. The Hamiltonian for this configuration can be written

$$H = \hbar\omega a^\dagger a + \hbar\omega_{eg} \sum_{m_e} |J_e m_e\rangle\langle J_e m_e| - i\hbar g(t) \left( a^\dagger A_0 - A_0^\dagger a \right) + i\hbar\Omega(t) \left( A_{+1} - A_{+1}^\dagger \right), \quad (8)$$

where the atomic lowering operators  $A_\sigma$  are given by

$$A_\sigma = \sum_{m_e, m_g} |J_g m_g\rangle\langle J_g m_g; 1\sigma|J_e m_e\rangle\langle J_e m_e|, \quad (9)$$

with  $\langle J_g m_g; 1\sigma|J_e m_e\rangle$  the Clebsch-Gordan coefficient for the dipole transition  $|e\rangle \rightarrow |g\rangle$  with polarization  $\sigma = 0, \pm 1$ .

If we consider the case in which the atom is initially in the state  $|g_{-N}\rangle$ , then the relevant adiabatic-following eigenstate (with eigenvalue  $E_n = n\hbar\omega$ ) of the above Hamiltonian takes the form

$$|E_n, g_{-N}\rangle = \mathcal{N} \{ |g_{-N}, n\rangle G_{-N+1}^{(n)} G_{-N+2}^{(n)} \cdots G_{N-1}^{(n)} + |g_{-N+1}, n+1\rangle \Omega_{-N+1} G_{-N+2}^{(n)} \cdots G_{N-1}^{(n)} + \cdots + |g_{N-1}, n+2N-1\rangle \times \Omega_{-N+1} \Omega_{-N+2} \cdots \Omega_{N-1} \}, \quad (10)$$

where

$$G_k^{(n)} = g(t) \sqrt{n+N+k} \langle J_g(m_g = k); 10|J_e(m_e = k)\rangle \quad (k < N), \quad (11)$$

$$\Omega_k = \Omega(t) \langle J_g(m_g = k-1); 11|J_e(m_e = k)\rangle \quad (k > -N), \quad (12)$$

and  $\mathcal{N}$  is a normalization factor. Hence, given that the atom is prepared in the state  $|g_{-N}\rangle$  and that one has an appropriate pulse sequence, in which  $g(t)$  precedes

$\Omega(t)$ , adiabatic passage along this dark state produces the transformation

$$|g_{-N}, n\rangle \longrightarrow |g_{N-1}, n + 2N - 1\rangle. \quad (13)$$

Such a transformation is depicted in Fig. 2(a) for an atomic  $J_g = 2 \rightarrow J_e = 1$  transition. In words, population initially in the atomic state  $|g_{-N}\rangle$  is coherently transferred to the state  $|g_{N-1}\rangle$  and the initial cavity mode state  $|n\rangle$  is transformed into the state  $|n+2N-1\rangle$ . Hence, for an initial vacuum state of the cavity mode, passage of a single atom yields a  $(2N-1)$ -photon Fock state in the cavity and each subsequent atom (entering in the state  $|g_{-N}\rangle$ ) increases the photon number by  $(2N-1)$ . Taking into consideration cavity losses, a single atom producing a  $(2N-1)$ -photon shift clearly has an advantage over a sequence of  $(2N-1)$  atoms each producing only a single-photon shift as described in Sec. II A 3.

### C. Orthogonal families of states

When the cavity is initially in the vacuum state, there exists the possibility of performing adiabatic passage

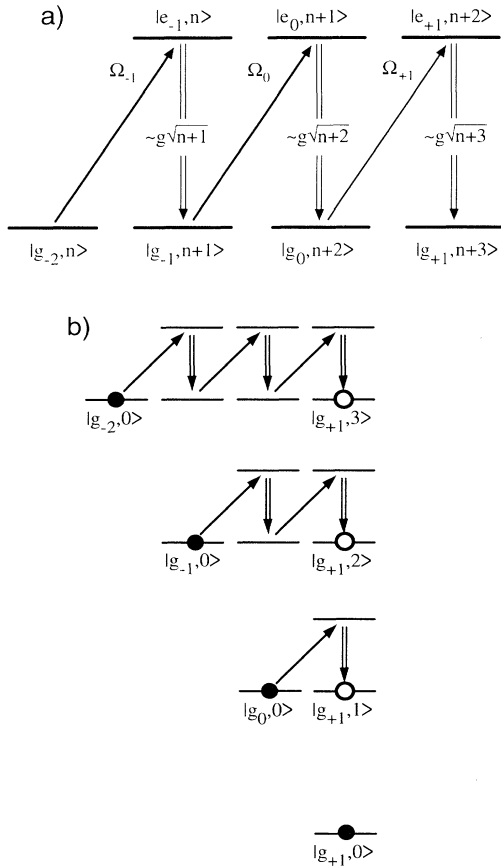


FIG. 2. (a) Depiction of the three-photon shift produced with an atomic  $J_g = 2 \rightarrow J_e = 1$  transition. (b) Depiction of the dependence of the shift of an initial vacuum cavity field on the initial atomic state. For the atomic  $J_g = 2 \rightarrow J_e = 1$  transition considered, shifts of zero, one, two, or three photons occur for the initial atomic states  $|g_{+1}\rangle$ ,  $|g_0\rangle$ ,  $|g_{-1}\rangle$ , or  $|g_{-2}\rangle$ , respectively.

with initial atomic states other than  $|g_{-N}\rangle$ . Each of the states  $|g_m, 0\rangle$  ( $m = -N, -N+1, \dots, N-1$ ) is associated with a different manifold of the system Hamiltonian. Each of these (orthogonal) manifolds possesses an independently evolving dark state of the form given above, asymptotically linking each state  $|g_m, 0\rangle$  with a unique Fock state of the field, i.e., via adiabatic passage one can generate the transformation

$$|g_m, 0\rangle \longrightarrow |g_{N-1}, N - m - 1\rangle. \quad (14)$$

Taking the example of a  $J_g = 2 \rightarrow J_e = 1$  transition ( $N = 2$ ), it follows that, in addition to performing adiabatic passage from the state  $|g_{-2}, 0\rangle$  (producing a three-photon Fock state) one can also consider adiabatic passage with initial state  $|g_{-1}, 0\rangle$ , which yields a two-photon Fock state, or with the initial states  $|g_0, 0\rangle$  and  $|g_{+1}, 0\rangle$ , which lead to the one-photon and vacuum Fock states, respectively. These four distinct possibilities are depicted in Fig. 2(b).

### D. Conditions for adiabatic passage

Until now, we have only specified that the evolution of the system be sufficiently slow in order for adiabatic passage to occur. Quantitative estimates of the restrictions on various parameters can be obtained as in Refs. [23,24]. Assuming Gaussian pulse profiles for  $\Omega(t)$  and  $g(t)$  of width  $T$  [full width at half maximum (FWHM)] and peak intensities  $\Omega_{max}$  and  $g_{max}$ , the necessary condition for adiabatic following is

$$\Omega_{max} T, 2g_{max} \sqrt{n+1} T \gg 1. \quad (15)$$

This condition results from the requirement that the probability for transitions from  $|E_n\rangle$  to other states be very small. Given that the pulses have a significant overlap in time, it ensures that  $|E_n\rangle$  is well separated from  $|E_n^\pm\rangle$  throughout the interaction and that nonadiabatic coupling between these eigenstates is not significant.

The conditions above minimize the probability for nonadiabatic transitions within a particular manifold. Dissipative effects due to cavity losses and atomic spontaneous emission can, on the other hand, lead to transitions between different manifolds of the system. As alluded to earlier, the technique of adiabatic passage is robust against the effects of spontaneous emission as, in principle, the excited atomic state is never populated. Of course, in practice some fraction of the population does reach the excited atomic state and hence large values of  $g_{max}$  and  $\Omega_{max}$  relative to the atomic spontaneous rate  $\Gamma$  are desirable.

Cavity damping cannot, of course, be avoided in the way that spontaneous emission is avoided. The effects of cavity dissipation come into play as soon as the cavity mode is excited. This means that before the adiabatic transfer is complete, photons may be emitted from the cavity, limiting the maximum number of intracavity photons at any one time. The effect of cavity dissipation is clearly to couple manifolds  $\{|g_1, n\rangle, |e, n\rangle, |g_2, n+1\rangle\}$  or different  $n$ : ideal adiabatic transfer occurs when the pas-

sage is across a single manifold.

Summarizing, the adiabatic passage technique will be optimized when

$$\Omega_{max}, g_{max} \gg \frac{1}{T} \gg n_{max}\kappa, \Gamma, \quad (16)$$

where  $\kappa$  is the cavity linewidth (FWHM) and  $n_{max}$  is the maximum photon number attained by the cavity mode. With respect to the condition on  $g_{max}$ , it is clear that we require conditions under which “vacuum Rabi splitting” would be observable in the coupled atom-cavity system [7–9].

Finally, it is important to note that, because of the adiabatic nature of the transformation we employ, the conditions for successful operation take the form of *inequalities* and hence the scheme is robust against small changes in the various parameters, i.e., precise values of coupling strengths and interaction times, etc., are not required for the scheme to operate. This tolerance of variations in parameter values is particularly appealing from the point of view of experiments.

### III. SHIFTING PHOTON DISTRIBUTIONS: NUMERICAL RESULTS

#### A. Master equation

For a realistic description of the atom-cavity system, in which dissipative channels are accounted for, we must employ a master equation description. Remaining with the case of an atomic  $J_g = N \rightarrow J_e = N - 1$  transition and with a  $\pi$ -polarized cavity-mode field and a  $\sigma^+$ -polarized laser field, the relevant master equation can be written in the form

$$\frac{\partial \rho}{\partial t} = -i(H_{eff}\rho - \text{H.c.}) + \Gamma \sum_{\sigma=0,\pm 1} A_\sigma \rho A_\sigma^\dagger + \kappa a \rho a^\dagger, \quad (17)$$

where  $\rho(t)$  is the reduced density operator of the system, and

$$H_{eff} = (\Delta - i\Gamma/2) \sum_{m_e} |J_e m_e\rangle \langle J_e m_e| - i\frac{\kappa}{2} a^\dagger a - i\Omega(t)(A_{+1} - A_{+1}^\dagger) + ig(t)(a^\dagger A_0 - A_0^\dagger a), \quad (18)$$

where now we have moved to a frame rotating at the laser frequency, which is assumed to be resonant with the cavity-mode frequency.

#### B. Mean photon number, photon-number variance, and atomic ground-state populations

In the following, we study the time evolution of the mean cavity photon number and the Mandel  $Q$  parameter (i.e., photon-number variance) and give the final atomic ground-state populations, obtained from numerical integration of the master equation given above. Our aim is to gauge the effectiveness of the adiabatic passage scheme

given realistic parameters. We concentrate in particular on the atom-cavity coupling strength  $g_{max}$  and the cavity-mode decay rate  $\kappa$ , since the maximization and minimization of these parameters respectively pose the most difficult challenges for experiments. Thus it is important to know magnitudes of these parameters required to produce interesting results.

Considerably more freedom is available to experimentalists with respect to the laser-field strength and the time delay (or physical overlap) between the cavity and laser fields. The values that we choose for these parameters approximately optimize the results in each case, although a reasonable variation is tolerable. For example, given a pulse width  $T = 1$  (FWHM) for both cavity and laser fields (as we choose below), a time delay  $\tau \simeq 0.6 - 0.8$  is found to give optimal results [26]. In all cases below, we use a delay  $\tau = 0.6$ , with the Gaussian pulses  $g(t)$  and  $\Omega(t)$  centered at  $t = 1.7$  and  $2.3$ , respectively. For the laser-field Rabi frequency we choose  $\Omega_{max} = 50$ , but a variation of 10–20 % in this value makes little difference to the results. A limited increase in the value of  $\Omega_{max}$  will usually improve the results somewhat, but if  $\Omega_{max}$  is too large relative to  $g_{max}$ , the adiabatic transfer is degraded. The atomic linewidth is taken to be  $\Gamma = 5$  and the cavity-mode and laser frequencies are assumed to be resonant with the atomic transition throughout all of the calculations that follow.

#### 1. Effect of atom-cavity coupling strength

For atomic transitions we consider just the two cases  $J_g = 1 \rightarrow J_e = 0$  and  $J_g = 4 \rightarrow J_e = 3$ . The latter case is relevant to cesium while the former, although possibly applicable to helium for instance, is included primarily to enable a comparison between results obtained for atomic transitions having different numbers of levels (and different Clebsch-Gordan coefficients). Four values of the coupling parameter  $g_{max}$  are studied and the ratios of these values to the atomic spontaneous emission rate  $\Gamma$  and the cavity-mode decay rate  $\kappa$  are  $g_{max} : \Gamma : \kappa = (10, 15, 20, 30) : 5 : 1$ . In recent experiments a ratio  $g_{max} : \Gamma : \kappa \simeq 7.2 : 5 : 1.2$  has been achieved with cesium atoms and an optical cavity mode [27]. Further improvements can be contemplated and so our choice of parameters seems reasonable.

The cavity mode is assumed to be initially in the vacuum state and the initial atomic state is taken to be  $|g_{-1}\rangle$  for the  $J_g = 1 \rightarrow J_e = 0$  transition and either  $|g_{-4}\rangle$  or  $|g_0\rangle$  for the  $J_g = 4 \rightarrow J_e = 3$  transition. Hence, under ideal conditions these three configurations would generate the cavity-mode Fock states  $|1\rangle$ ,  $|7\rangle$ , and  $|3\rangle$ , respectively.

In Figs. 3–5 we plot the mean cavity photon number  $\langle n \rangle = \langle a^\dagger a \rangle$  and the Mandel  $Q$  parameter

$$Q = \frac{\langle (a^\dagger a)^2 \rangle - \langle a^\dagger a \rangle^2}{\langle a^\dagger a \rangle} - 1 \quad (19)$$

as a function of time. Tables I–III give the final atomic ground-state populations following the passage of the

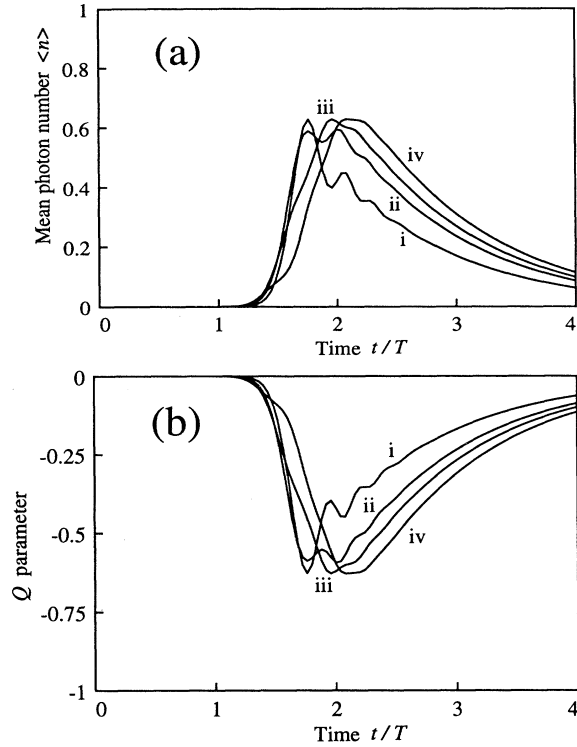


FIG. 3. (a) Mean cavity-mode photon number  $\langle n \rangle$  and (b) cavity-field Mandel  $Q$  parameter as a function of time for an atomic  $J_g = 1 \rightarrow J_e = 0$  transition. The initial system state is  $|g_{-1}\rangle \otimes |0\rangle$  and parameters are  $\Gamma = 5$ ,  $\kappa = 1$ ,  $\Omega_{max} = 50$ , and  $g_{max} = 10$  (i), 15 (ii), 20 (iii), and 30 (iv).

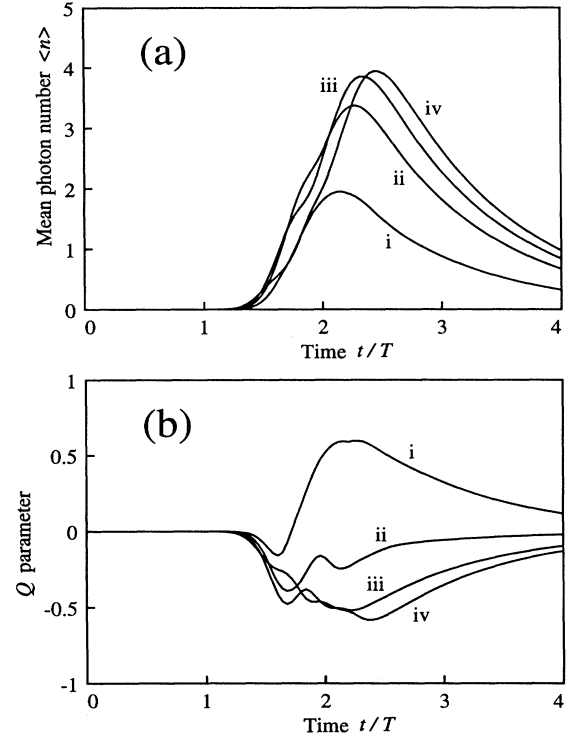


FIG. 4. (a) Mean cavity-mode photon number  $\langle n \rangle$  and (b) cavity-field Mandel  $Q$  parameter as a function of time for an atomic  $J_g = 4 \rightarrow J_e = 3$  transition. The initial system state is  $|g_{-4}\rangle \otimes |0\rangle$  and parameters are  $\Gamma = 5$ ,  $\kappa = 1$ ,  $\Omega_{max} = 50$ , and  $g_{max} = 10$  (i), 15 (ii), 20 (iii), and 30 (iv).

atom through the interaction region. For a  $J_g = N \rightarrow J_e = N - 1$  transition, with ideal conditions, all atomic population should be transferred to the state  $|g_{+N-1}\rangle$ . In the tables, the populations of the other ground-state sublevels give an indication of how well adiabatic passage is operating, with, in particular, the population of the state  $|g_{+N}\rangle$  giving some measure of the influence of atomic spontaneous emission (since this state can only be reached via spontaneous emission).

The major features demonstrated by these results can be summarized as follows.

(i) The greater the number of states involved in the adiabatic transformation, the more critical the value of  $g_{max}$  is. For the  $J_g = 1 \rightarrow J_e = 0$  transition, reason-

TABLE I. Atomic ground-state populations following adiabatic passage for a  $J_g = 1 \rightarrow J_e = 0$  atomic transition with initial atomic state  $|g_{-1}\rangle$ . The parameters are as in Fig. 3.

Coupling strength $g_{max}$	Atomic ground-state populations		
	$ g_{-1}\rangle$	$ g_0\rangle$	$ g_{+1}\rangle$
10	0.006	0.840	0.154
15	0.001	0.945	0.054
20	0.000	0.975	0.025
30	0.000	0.989	0.011

able results (with respect to atomic population transfer and maximum mean photon number and minimum  $Q$  parameter attained) are obtained even for  $g_{max} = 10$ . The same can be said for the  $J_g = 4 \rightarrow J_e = 3$  transition with initial state  $|g_0\rangle$ , but with initial state  $|g_{-4}\rangle$ ,  $g_{max} = 10$  is clearly too small to yield efficient transfer. Of course, the actual coupling parameter between the cavity mode and the dipole transition between a pair of Zeeman sublevels is proportional to the Clebsch-Gordan coefficient for this transition. For high- $J$  atomic levels Clebsch-Gordan coefficients can be small, reducing the effective coupling to the cavity mode and putting greater demands on the value of  $g_{max}$  required for adiabatic passage. A minimum value  $g_{max} \simeq 15 - 20$  is seen to be necessary for the  $J_g = 4 \rightarrow J_e = 3$  transition with initial state  $|g_{-4}\rangle$ .

(ii) Beyond a certain value of  $g_{max}$  the results do not improve significantly. Some further improvement is possible with an increase in the laser-field strength (again though, an optimum value of  $\Omega_{max}$  is reached, beyond which the results do not improve), but the optimum attainable values of the mean photon number  $\langle n \rangle$  and  $Q$  parameter are ultimately limited by cavity dissipation. A decrease in the interaction time can obviously counteract this effect, but a corresponding increase in the coupling parameter  $g_{max}$  is necessary in order to satisfy the adiabatic passage condition  $g_{max}T \gg 1$ .

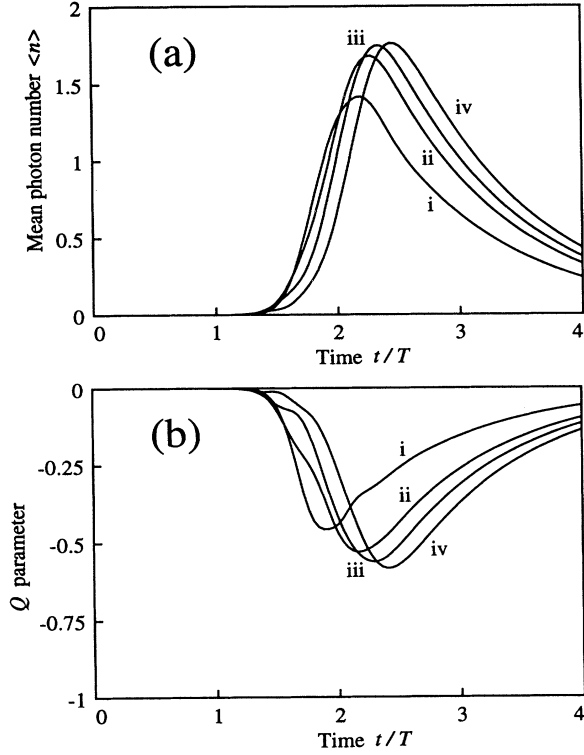


FIG. 5. (a) Mean cavity-mode photon number  $\langle n \rangle$  and (b) cavity-field Mandel  $Q$  parameter as a function of time for an atomic  $J_g = 4 \rightarrow J_e = 3$  transition. The initial system state is  $|g_0\rangle \otimes |0\rangle$  and parameters are  $\Gamma = 5$ ,  $\kappa = 1$ ,  $\Omega_{max} = 50$ , and  $g_{max} = 10$  (i), 15 (ii), 20 (iii), and 30 (iv).

## 2. Effect of cavity damping

For our next series of figures (Figs. 6–8) and tables (Tables IV–VI), we fix the parameter  $g_{max}$  (to a value which, in Sec. III B 1, enabled a good adiabatic transfer) and consider the effect of varying the cavity-mode decay rate  $\kappa$ . The parameter ratios we consider are  $g_{max} : \Gamma : \kappa = 20 : 5 : (0, 0.25, 0.50, 1.0)$  and the three configurations we examine are as described above.

The essential features of the results are as follows.

(i) As one would expect, increasing the rate  $\kappa$  degrades the optimal attainable values of  $\langle n \rangle$  and  $Q$ .

(ii) From the final atomic ground-state populations, one sees that varying the magnitude of  $\kappa$  has little effect on atomic population transfer in these configurations. To some extent, cavity dissipation can be regarded as a pro-

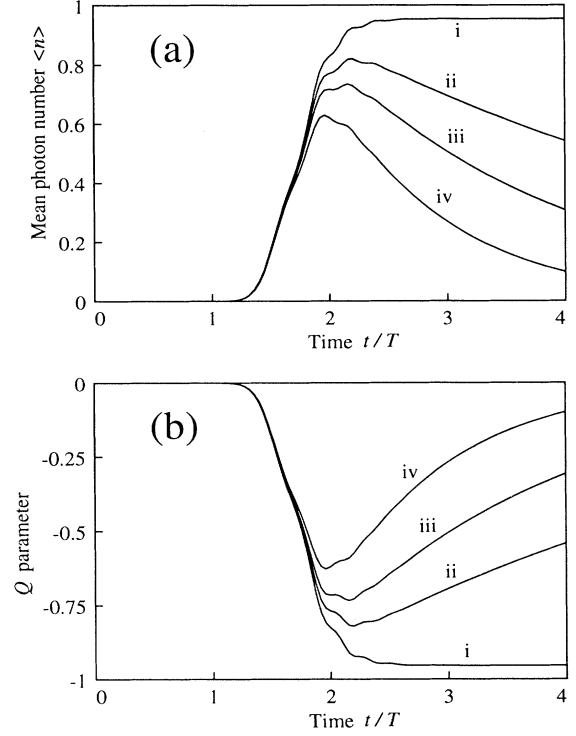


FIG. 6. (a) Mean cavity-mode photon number  $\langle n \rangle$  and (b) cavity-field Mandel  $Q$  parameter as a function of time for an atomic  $J_g = 1 \rightarrow J_e = 0$  transition. The initial system state is  $|g_{-1}\rangle \otimes |0\rangle$  and parameters are  $\Gamma = 5$ ,  $g_{max} = 20$ ,  $\Omega_{max} = 50$ , and  $\kappa = 0$  (i), 0.25 (ii), 0.5 (iii), and 1.0 (iv).

cess operating independently of adiabatic passage. While photon emissions from the cavity may cause jumps between different “families” of states of the system, they do not necessarily inhibit the adiabatic transfer process; it is possible that a jump effectively “shifts” the adiabatic transfer to another dark state. However, for sufficiently large values of  $\kappa$  (e.g.,  $\kappa \geq 10$ ), calculations show that adiabatic transfer no longer operates efficiently. Of course, in the limit of large  $\kappa$  (i.e., in the bad cavity regime, where the cavity field can be adiabatically eliminated from the dynamics), the effect of the cavity is simply to enhance the atomic spontaneous emission rate. Our system can then be described in terms of a laser-driven atom with a modified spontaneous emission rate [28], resulting merely in optical pumping of the atom into the states  $|g_{+N-1}\rangle$  and  $|g_{+N}\rangle$ .

TABLE II. Atomic ground-state populations following adiabatic passage for a  $J_g = 4 \rightarrow J_e = 3$  atomic transition with initial atomic state  $|g_{-4}\rangle$ . The parameters are as in Fig. 4.

Coupling strength	Atomic ground-state populations									
	$g_{max}$	$ g_{-4}\rangle$	$ g_{-3}\rangle$	$ g_{-2}\rangle$	$ g_{-1}\rangle$	$ g_0\rangle$	$ g_{+1}\rangle$	$ g_{+2}\rangle$	$ g_{+3}\rangle$	$ g_{+4}\rangle$
10		0.068	0.066	0.063	0.063	0.062	0.063	0.074	0.358	0.183
15		0.014	0.015	0.015	0.017	0.018	0.021	0.031	0.701	0.168
20		0.002	0.002	0.002	0.003	0.004	0.005	0.014	0.812	0.156
30		0.000	0.000	0.000	0.000	0.001	0.002	0.008	0.812	0.176

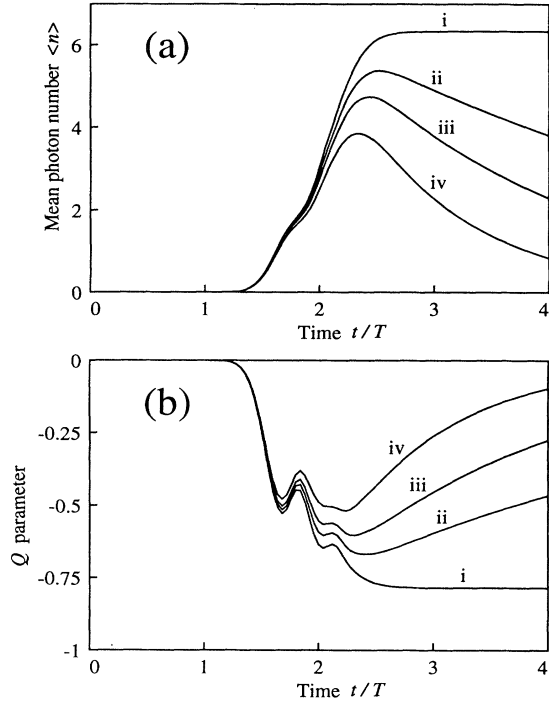


FIG. 7. (a) Mean cavity-mode photon number  $\langle n \rangle$  and (b) cavity-field Mandel  $Q$  parameter as a function of time for an atomic  $J_g = 4 \rightarrow J_e = 3$  transition. The initial system state is  $|g_{-4}\rangle \otimes |0\rangle$  and parameters are  $\Gamma = 5$ ,  $g_{max} = 20$ ,  $\Omega_{max} = 50$ , and  $\kappa = 0$  (i), 0.25 (ii), 0.5 (iii), and 1.0 (iv).

### C. Photon-counting distributions

The most direct approach to detecting Fock states produced by adiabatic passage is to perform photon-counting measurements on the field leaking from the cavity through the mirrors. In the ideal scenario, these measurements would be conditioned upon the transit of an atom through the cavity, thereby avoiding complications associated with atomic-number fluctuations and realizing a clean single-atom experiment. Though difficult, such a scenario appears to be within reach of experimentalists and we will assume this ideal situation in the calculations that follow. We will return briefly to this point in the Conclusion and describe a possible experimental configuration.

TABLE III. Atomic ground-state populations following adiabatic passage for a  $J_g = 4 \rightarrow J_e = 3$  atomic transition with initial atomic state  $|g_0\rangle$ . The parameters are as in Fig. 5.

Coupling strength $g_{max}$	Atomic ground-state populations				
	$ g_0\rangle$	$ g_{+1}\rangle$	$ g_{+2}\rangle$	$ g_{+3}\rangle$	$ g_{+4}\rangle$
10	0.000	0.001	0.009	0.733	0.257
15	0.000	0.000	0.007	0.852	0.140
20	0.000	0.000	0.005	0.882	0.113
30	0.000	0.000	0.004	0.884	0.112

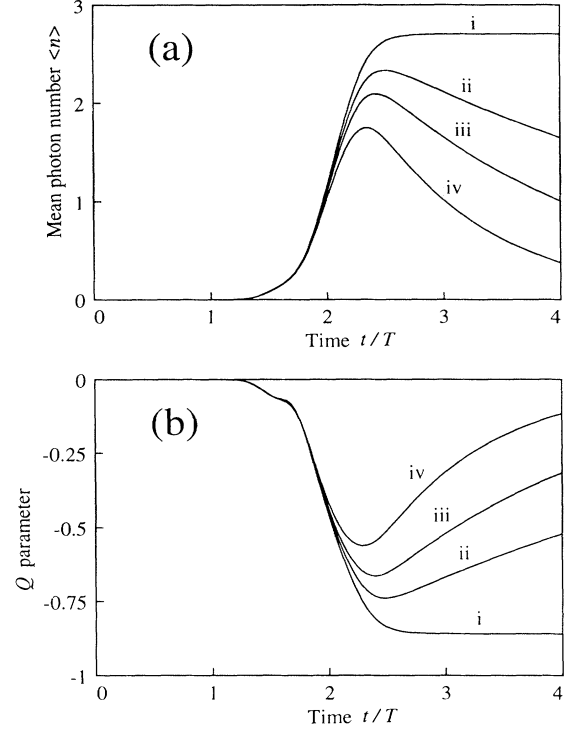


FIG. 8. (a) Mean cavity-mode photon number  $\langle n \rangle$  and (b) cavity-field Mandel  $Q$  parameter as a function of time for an atomic  $J_g = 4 \rightarrow J_e = 3$  transition. The initial system state is  $|g_0\rangle \otimes |0\rangle$  and parameters are  $\Gamma = 5$ ,  $g_{max} = 20$ ,  $\Omega_{max} = 50$ , and  $\kappa = 0$  (i), 0.25 (ii), 0.5 (iii), and 1.0 (iv).

#### 1. Monte Carlo wave-function simulations

The recently developed theoretical technique of quantum Monte Carlo wave-function simulation [29–31] is ideally suited to the study of photon-counting measurements of the field emitted from the cavity. This technique consists of system wave-function propagation with a non-Hermitian (damped) system Hamiltonian, interrupted at random times by wave-function collapses, or quantum jumps, which can be interpreted as, for instance, emissions of photons from atoms or cavities. In the present context, photon-counting distributions can be computed very straightforwardly by simulating the passage of many atoms through the cavity and counting cavity emissions

TABLE IV. Atomic ground-state populations following adiabatic passage for a  $J_g = 1 \rightarrow J_e = 0$  atomic transition with initial atomic state  $|g_{-1}\rangle$ . The parameters are as in Fig. 6.

Cavity linewidth $\kappa$	Atomic ground-state populations		
	$ g_{-1}\rangle$	$ g_0\rangle$	$ g_{+1}\rangle$
0.00	0.000	0.977	0.023
0.25	0.000	0.977	0.023
0.50	0.000	0.976	0.024
1.00	0.000	0.975	0.025

TABLE V. Atomic ground-state populations following adiabatic passage for a  $J_g = 4 \rightarrow J_e = 3$  atomic transition with initial atomic state  $|g_{-4}\rangle$ . The parameters are as in Fig. 7.

Cavity linewidth $\kappa$	Atomic ground-state populations								
	$ g_{-4}\rangle$	$ g_{-3}\rangle$	$ g_{-2}\rangle$	$ g_{-1}\rangle$	$ g_0\rangle$	$ g_{+1}\rangle$	$ g_{+2}\rangle$	$ g_{+3}\rangle$	$ g_{+4}\rangle$
0.00	0.002	0.002	0.002	0.003	0.003	0.005	0.018	0.825	0.141
0.25	0.002	0.002	0.002	0.003	0.003	0.005	0.016	0.823	0.144
0.50	0.002	0.002	0.002	0.003	0.004	0.005	0.015	0.820	0.147
1.00	0.002	0.002	0.002	0.003	0.004	0.005	0.014	0.812	0.156

per atom. Details of the method are given in the Appendix.

As mentioned above, we assume that the detection interval is conditioned (or “triggered”) by the arrival of an atom. The detection interval itself is typically ten or more cavity lifetimes, i.e., we count emissions until such a time that the probability for further emissions is negligible. Repeating this procedure for many atoms, we generate a probability distribution  $P(n)$  for detecting  $n$  photons per atom, given perfect detector efficiency. To account for nonunit detector efficiency, we simply apply the formula

$$P(n, e) = \sum_{m=n}^{\infty} P(m) \frac{m!}{n!(m-n)!} e^n (1-e)^{m-n}, \quad (20)$$

which gives the probability distribution  $P(n, e)$  for the detection of  $n$  photons given that the efficiency is  $e$  ( $0 \leq e \leq 1$ ).

## 2. Results

We confine ourselves to a  $J_g = 4 \rightarrow J_e = 3$  atomic transition, as this is of most relevance to experiments using cesium atoms. The pulse widths and separation are given their (approximately) optimal values and we consider values of the coupling strength  $g_{max}$  and cavity linewidth  $\kappa$  which, we believe, are within reach of present experiments. The photon-counting distributions are formed from ensembles of 2000 atoms — this number is sufficient to produce reliable statistics. As initial atomic states, we choose  $|g_{-4}\rangle$  and  $|g_0\rangle$ , which under ideal conditions would lead to the generation of the cavity-mode Fock states  $|7\rangle$  and  $|3\rangle$ , respectively.

In Tables VII and VIII we give the computed probability distributions for these two cases, together with the mean number of detected photons  $\langle n \rangle = \sum nP(n, e)$  and the  $Q$  parameter, computed from

$$Q = \frac{\langle n^2 \rangle - \langle n \rangle^2}{\langle n \rangle} - 1, \quad (21)$$

with  $\langle n^2 \rangle = \sum n^2 P(n, e)$ . Negative values of  $Q$  signify a nonclassical photon distribution. Three values of the photon-counting detector efficiency are considered,  $e = 0.3, 0.6, 1.0$ .

In all cases, one sees that, for the majority of atoms, seven (initial state  $|g_{-4}\rangle$ ) or three (initial state  $|g_0\rangle$ ) photons are emitted from the cavity. Nonunit detector efficiency obviously reduces the observed number, but significantly negative values of the  $Q$  parameter persist. With photon detectors of  $\sim 70$ – $80\%$  efficiency now available [32], detector efficiency should not pose a major practical barrier to the observation of nonclassical distributions.

The performance of the scheme is seen to be better for the case in which the initial atomic state is  $|g_0\rangle$ . As more atomic levels (and hence more Clebsch-Gordan coefficients) contribute to the adiabatic-following state, it becomes desirable to increase the coupling strength  $g_{max}$ .

For each case, we also consider two values of the cavity linewidth  $\kappa$ . We see that relatively large values of  $\kappa$  compared to  $g_{max}$  do not exclude the possibility of producing significantly nonclassical distributions and might actually be somewhat advantageous in terms of the length of the required detection interval.

Finally, Table IX shows results again for the initial state  $|g_0\rangle$ , but now with a reduced value of  $g_{max}$  compared to that of Tables VII and VIII. The effects are somewhat diminished compared with Table VIII, but still comparable in quality to those of Table VII (initial state  $|g_{-4}\rangle$ ), highlighting the previously mentioned point that the demands on the coupling strength  $g_{max}$  are less stringent for situations in which fewer states participate in the adiabatic passage process. For the case of a  $J_g = 4 \rightarrow J_e = 3$  transition, and from the point of view of experiments, it follows that some advantage is to be gained by considering adiabatic passage from the initial state  $|g_0\rangle$ .

## IV. COHERENT SUPERPOSITION STATES OF THE CAVITY FIELD

### A. Orthogonal families of states

In Ref. [19] it was pointed out that adiabatic passage in an atom-cavity system has the potential to generate not only Fock states of the cavity field, but also quite general superposition states. This potential arises from the existence of orthogonal manifolds of the system Hamil-

TABLE VI. Atomic ground-state populations following adiabatic passage for a  $J_g = 4 \rightarrow J_e = 3$  atomic transition with initial atomic state  $|g_0\rangle$ . The parameters are as in Fig. 8.

Cavity linewidth $\kappa$	Atomic ground-state populations				
	$ g_0\rangle$	$ g_{+1}\rangle$	$ g_{+2}\rangle$	$ g_{+3}\rangle$	$ g_{+4}\rangle$
0.00	0.000	0.000	0.008	0.890	0.101
0.25	0.000	0.000	0.007	0.889	0.104
0.50	0.000	0.000	0.006	0.887	0.107
1.00	0.000	0.000	0.005	0.882	0.113

TABLE VII. Probability distribution  $P(n, e)$  for the detection of  $n$  photons emitted from the cavity as a result of adiabatic passage with an atomic  $J_g = 4 \rightarrow J_e = 3$  atomic transition. The initial atomic state is  $|g_{-4}\rangle$ . Parameters are  $\Gamma = 5$ ,  $g_{max} = 20$ ,  $\Omega_{max} = 50$ , pulse width  $T = 1$ , and pulse separation  $\tau = 0.6$ . Three values of the detector efficiency  $e$  and two values of the cavity linewidth  $\kappa$  are considered.

$\kappa$	$e$	$P(0, e)$	$P(1, e)$	$P(2, e)$	$P(3, e)$	$P(4, e)$	$P(5, e)$	$P(6, e)$	$P(7, e)$	$\langle n \rangle$	$Q$
1.0	0.3	0.120	0.282	0.309	0.194	0.075	0.018	0.002	0.000	1.89	-0.236
	0.6	0.012	0.045	0.125	0.231	0.275	0.206	0.089	0.017	3.77	-0.472
	1.0	0.003	0.007	0.007	0.018	0.040	0.101	0.224	0.600	6.28	-0.787
5.0	0.3	0.151	0.299	0.298	0.174	0.062	0.014	0.002	0.000	1.75	-0.189
	0.6	0.027	0.067	0.150	0.243	0.259	0.174	0.068	0.012	3.49	-0.379
	1.0	0.010	0.017	0.018	0.027	0.072	0.151	0.289	0.416	5.82	-0.631

tonian associated with each of the states  $|g_m, 0\rangle$  ( $m = -N, -N+1, \dots, N-1$ ), as described earlier in Sec. II C. Because of the orthogonality of the manifolds, the different states  $|g_m, 0\rangle$  evolve, under adiabatic-following conditions, entirely independently of each other. It follows that any initial coherent superposition of atomic ground-state Zeeman sublevels will be mapped onto an equivalent coherent superposition of cavity-mode Fock states. This is represented, for a  $J_g = N \rightarrow J_e = N-1$  atomic transition, by the transformation equation

$$\sum_{m=-N}^{N-1} c_m |g_m\rangle \otimes |0\rangle \longrightarrow |g_{N-1}\rangle \otimes \sum_{m=-N}^{N-1} c_m |N-m-1\rangle. \quad (22)$$

Hence, to the extent that one can prepare arbitrary superpositions of atomic ground-state sublevels, one can also, in principle, prepare arbitrary superposition states of the cavity light field.

The implementation of such a transformation is illustrated in Figs. 9 and 10, where we plot histograms of the moduli of the cavity-mode density-matrix elements  $\langle n | \rho_f | m \rangle$  at a sequence of times during the passage of an atom (obtained from direct numerical solutions of the master equation). In this example, we consider a  $J_g = 4 \rightarrow J_e = 3$  atomic transition, with the atom initially prepared in the state  $2^{-1/2}(|g_0\rangle + |g_{+3}\rangle)$  and

the cavity initially in the vacuum state. The field superposition state that we attempt to generate is thus  $2^{-1/2}(|0\rangle + |3\rangle)$ . For the case  $\kappa = 0$  (Fig. 9) such a state is indeed seen to be produced, while for the case of non-zero cavity-mode dissipation the superposition does not reach its optimum form (Fig. 10). However, off-diagonal density-matrix terms do appear for significant periods of time, suggesting that signatures of quantum coherences should still be observable. The results to be presented in the following sections confirm this.

From an experimental point of view, several possibilities exist for the initial preparation of atomic ground-state superpositions. With an atom such as cesium, population can be optically pumped into the outermost Zeeman ground state or into the state  $m_g = 0$  with suitably tuned and polarized lasers. The coordinate axis for this optical pumping can be chosen to be different from that in the adiabatic passage interaction region: this yields initial atomic ground-state superpositions for the adiabatic transfer. Coherences between Zeeman sublevels could also be generated by employing radio-frequency pulses between sublevels or between sublevels of different hyperfine structure components.

## B. Photon-counting measurements

Although direct photon-counting measurements on the field emitted from the cavity cannot confirm the presence of coherent superposition states, it is nevertheless inter-

TABLE VIII. Probability distribution  $P(n, e)$  for the detection of  $n$  photons emitted from the cavity as a result of adiabatic passage with an atomic  $J_g = 4 \rightarrow J_e = 3$  atomic transition. The initial atomic state is  $|g_0\rangle$ . Parameters are  $\Gamma = 5$ ,  $g_{max} = 20$ ,  $\Omega_{max} = 50$ , pulse width  $T = 1$ , and pulse separation  $\tau = 0.6$ . Three values of the detector efficiency  $e$  and two values of the cavity linewidth  $\kappa$  are considered.

$\kappa$	$e$	$P(0, e)$	$P(1, e)$	$P(2, e)$	$P(3, e)$	$\langle n \rangle$	$Q$
1.0	0.3	0.394	0.425	0.160	0.021	0.808	-0.256
	0.6	0.109	0.334	0.390	0.167	1.62	-0.512
	1.0	0.010	0.060	0.156	0.774	2.69	-0.853
5.0	0.3	0.423	0.415	0.144	0.018	0.756	-0.234
	0.6	0.135	0.360	0.362	0.143	1.51	-0.468
	1.0	0.014	0.110	0.218	0.658	2.52	-0.779

TABLE IX. Probability distribution  $P(n, e)$  for the detection of  $n$  photons emitted from the cavity as a result of adiabatic passage with an atomic  $J_g = 4 \rightarrow J_e = 3$  atomic transition. The initial atomic state is  $|g_0\rangle$ . Parameters are  $\Gamma = 5$ ,  $g_{max} = 15$ ,  $\Omega_{max} = 50$ , pulse width  $T = 1$ , and pulse separation  $\tau = 0.6$ . Three values of the detector efficiency  $e$  and two values of the cavity linewidth  $\kappa$  are considered.

$\kappa$	$e$	$P(0, e)$	$P(1, e)$	$P(2, e)$	$P(3, e)$	$\langle n \rangle$	$Q$
1.0	0.3	0.423	0.414	0.145	0.018	0.759	-0.232
	0.6	0.136	0.355	0.364	0.145	1.52	-0.465
	1.0	0.018	0.107	0.202	0.673	2.53	-0.775
5.0	0.3	0.464	0.398	0.124	0.014	0.687	-0.206
	0.6	0.176	0.385	0.328	0.111	1.37	-0.412
	1.0	0.032	0.161	0.293	0.514	2.29	-0.687

esting to model the results one would expect to obtain from such measurements when the state being prepared is, for instance, a coherent superposition of Fock states. The photon-counting distribution should in such a case exhibit a double-peaked structure. Given that such a structure could be resolved, the superposed states could then be considered to be “macroscopically distinguishable” and subsequent demonstration of coherences (using, for example, the homodyne measurements described in the following subsection) could thus be judged to be a demonstration of a coherent superposition of macroscopically distinguishable states.

We present two examples for which the initial atomic states are  $2^{-1/2}(|g_{-4}\rangle + |g_{+3}\rangle)$  and  $2^{-1/2}(|g_0\rangle + |g_{+3}\rangle)$ , respectively, and the cavity mode is initially in the vacuum state. Hence, under ideal conditions, the Fock state

superpositions  $2^{-1/2}(|0\rangle + |7\rangle)$  and  $2^{-1/2}(|0\rangle + |3\rangle)$ , respectively, would be generated. Simulated photon distributions are given in Tables X and XI for possible experimental parameters and for different values of the photon-counting efficiency  $e$ . For the first example, a double-peaked structure in the photon distribution is still resolvable for  $e = 0.3$ . However, for the second example, where the separation between superposed states is not as large, this structure disappears much more rapidly as the efficiency is decreased.

### C. Homodyne measurements of the cavity field

The coherences that characterize quantum-mechanical superposition states would most directly be detected via homodyne measurements of the field exiting the cavity. A strong local oscillator field is mixed with the signal field (leaking from the cavity) and, for a particular phase

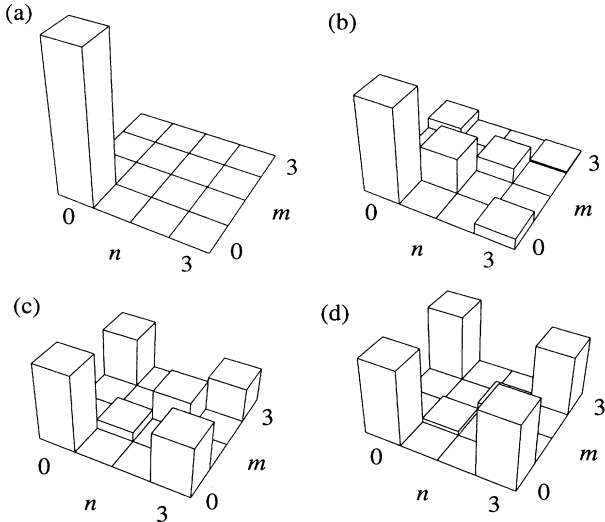


FIG. 9. Moduli of the cavity density matrix elements  $\langle n | \rho_{cav} | m \rangle$  at a sequence of times during adiabatic transfer. The atom is prepared in the state  $2^{-1/2}(|g_0\rangle + |g_{+3}\rangle)$  and relevant parameters are  $g_{max} = 20$ ,  $\Omega_{max} = 60$ ,  $\Gamma = 5$ , and  $\kappa = 0$ . The pulses  $g(t)$  and  $\Omega(t)$  are centered at  $t = 1.7$  and  $t = 2.3$ , respectively, and each have a width  $T = 1$ . The moduli are shown at times (a)  $t = 0$ , (b)  $t = 1.9$ , (c)  $t = 2.2$ , and (d)  $t = 2.7$ .

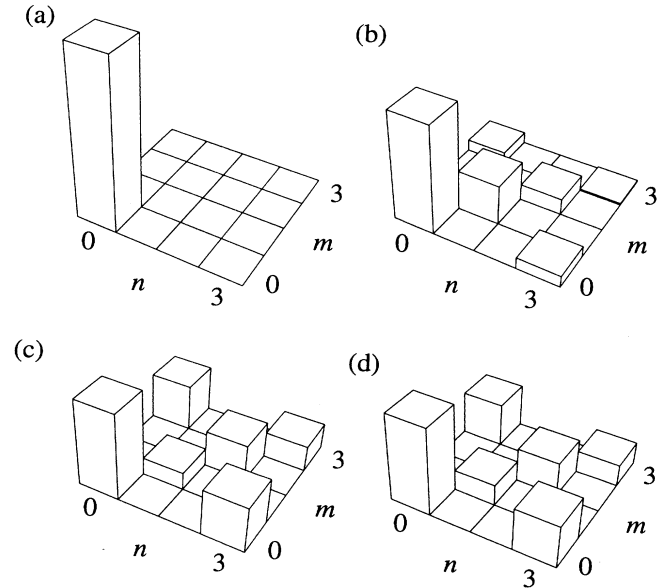


FIG. 10. Moduli of the cavity density matrix elements  $\langle n | \rho_{cav} | m \rangle$  for the parameters of Fig. 9, but with  $\kappa = 0.5$ . The moduli are shown at times (a)  $t = 0$ , (b)  $t = 1.9$ , (c)  $t = 2.2$ , and (d)  $t = 2.7$ .

TABLE X. Probability distribution  $P(n, e)$  for the detection of  $n$  photons emitted from the cavity as a result of adiabatic passage with an atomic  $J_g = 4 \rightarrow J_e = 3$  atomic transition. The initial atomic state is  $2^{-1/2}(|g_{-4}\rangle + |g_{+3}\rangle)$ . Parameters are  $\Gamma = 5$ ,  $g_{max} = 20$ ,  $\kappa = 1.0$ ,  $\Omega_{max} = 50$ , pulse width  $T = 1$ , and pulse separation  $\tau = 0.6$ . Three values of the detector efficiency  $e$  are considered.

$e$	$P(0, e)$	$P(1, e)$	$P(2, e)$	$P(3, e)$	$P(4, e)$	$P(5, e)$	$P(6, e)$	$P(7, e)$
0.3	0.571	0.136	0.151	0.095	0.037	0.009	0.001	0.000
0.6	0.520	0.020	0.060	0.112	0.135	0.101	0.044	0.008
1.0	0.517	0.001	0.001	0.011	0.018	0.042	0.118	0.292

$\theta$  of the local oscillator, one measures the probability distribution  $P(x_\theta)$  for the quadrature amplitude  $x_\theta$  of the signal field. Given that  $\rho_{cav}$  is the cavity-mode density matrix,  $P(x_\theta)$  can be expressed as

$$\begin{aligned}
 P(x_\theta) &= \langle x_\theta | \rho_{cav} | x_\theta \rangle \\
 &= \pi^{-1/2} \sum_{n,m} \rho_{nm} e^{i\theta(n-m)} (2^n n!)^{-1/2} (2^m m!)^{-1/2} \\
 &\quad \times H_n(x) H_m(x) e^{-x^2}, \quad (23)
 \end{aligned}$$

where  $\rho_{nm}$  are the elements of  $\rho_{cav}$  in the number-state basis and  $H_n(x)$  are the Hermite polynomials.

The proposed experimental procedure is as follows. Again, we assume that the measurement is in some way triggered by a signal from a single-atom detection scheme. The homodyne signal (current) is then integrated over a certain time interval  $(T_0, T_1)$ , which ideally should encompass the time during which quantum coherences are maximal. Carrying out this procedure for many atoms and for a particular local oscillator phase, one should generate a probability distribution in the manner of Smithey *et al.* [33]. This probability distribution should theoretically be of the form

$$P_I(x_\theta) \propto \int_{T_0}^{T_1} d\tau \langle x_\theta | \rho_{cav}(\tau) | x_\theta \rangle \equiv I_{hom}(x_\theta). \quad (24)$$

In the figures that follow we plot the integral  $I_{hom}(x)$ , which we compute from numerical solutions of the master equation.

We note that Monte Carlo wave-function simulations could also be employed to model homodyne measurements of the field and to perhaps give a more faithful model of actual experiments. Such models have been

TABLE XI. Probability distribution  $P(n, e)$  for the detection of  $n$  photons emitted from the cavity as a result of adiabatic passage with an atomic  $J_g = 4 \rightarrow J_e = 3$  atomic transition. The initial atomic state is  $2^{-1/2}(|g_0\rangle + |g_{+3}\rangle)$ . Parameters are  $\Gamma = 5$ ,  $g_{max} = 20$ ,  $\kappa = 1.0$ ,  $\Omega_{max} = 50$ , pulse width  $T = 1$ , and pulse separation  $\tau = 0.6$ . Three values of the detector efficiency  $e$  are considered.

$e$	$P(0, e)$	$P(1, e)$	$P(2, e)$	$P(3, e)$
0.3	0.708	0.206	0.076	0.010
0.6	0.568	0.166	0.188	0.078
1.0	0.517	0.034	0.087	0.362

discussed and studied in detail in Refs. [29,34], with careful consideration given to the actual measurement process (for instance, explicitly modeling local oscillator shot noise).

### 1. Superposition of Fock states

We consider again the example given at the beginning of this section, for which the ‘‘ideal’’ transformation has the form

$$2^{-1/2}(|g_0\rangle + |g_{+3}\rangle) \otimes |0\rangle \longrightarrow |g_{+3}\rangle \otimes 2^{-1/2}(|0\rangle + |3\rangle). \quad (25)$$

In Figs. 11(a) and 11(b),  $I_{hom}(x_\theta)$  is plotted for the three choices of phase  $\theta = 0, \pi/6, \pi/3$  and for two integration intervals  $(T_0, T_1)$ .

The ‘‘idealized’’ result, obtained in the limit  $\kappa \rightarrow 0$ , is shown in Fig. 11(c). The case  $\theta = \pi/6$  yields the same result as for the incoherent mixture  $2^{-1/2}(|0\rangle\langle 0| + |3\rangle\langle 3|)$  and the structure of  $I_{hom}(x)$  is very close to that of the Fock state  $|3\rangle$ . For the other cases,  $\theta = 0, \pi/3$ , one sees the effects of interference caused by the quantum-mechanical coherences.

With potential experimental parameters these features are not as pronounced [Figs. 11(a) and 11(b)], but the basic structure persists. The results can be optimized with a judicious choice of the integration interval, but there seems to be a reasonably wide range of times over which the effects can still be observed.

### 2. Superposition of coherent states

Because of its close correspondence to the classical description of harmonic physics, the coherent state arises naturally in discussions of schemes for the generation of superpositions of classically distinguishable quantum states. Here we can also consider superpositions of coherent states, although the coherent state amplitude is for our scheme limited by the finite degeneracy of the atomic ground state. In particular, we consider injecting atoms prepared in an initial state of the form

$$\mathcal{N} e^{-|\alpha|^2/2} \left( \alpha |g_{+2}\rangle + \frac{\alpha^3}{\sqrt{3!}} |g_0\rangle + \frac{\alpha^5}{\sqrt{5!}} |g_{-2}\rangle + \frac{\alpha^7}{\sqrt{7!}} |g_{-4}\rangle \right), \quad (26)$$

where  $\mathcal{N}$  is a normalization factor. Provided  $\alpha$  is not too large, adiabatic passage will generate the cavity mode superposition state

$$\mathcal{N}' (|\alpha\rangle - |-\alpha\rangle), \quad (27)$$

where  $|\alpha\rangle$  is the coherent state with amplitude  $\alpha$ . For the particular atomic transition considered here, we are limited to  $\alpha \approx \sqrt{2}$ , so the superposed states will at most be separated by a distance in the complex-amplitude plane corresponding to only a few quanta (i.e., Schrödinger “kittens” [35]).

The parameter set we consider in Fig. 12 is the same

as for Figs. 11(a) and 11(c), with the idealized result ( $\kappa \rightarrow 0$ ) again given in Fig. 12(c). The value for the coherent amplitude is taken to be  $\alpha = \sqrt{2}$ . For  $\theta = 0$ , one sees the distributions of two classical states, while for  $\theta = \pi/2$  interference fringes appear signifying quantum coherences between these states and in particular the existence of a coherent superposition state. For nonzero cavity dissipation these features are degraded compared to the idealized result; the separation between the two “classical” distributions for  $\theta = 0$  is reduced and the interference fringes are not as pronounced. However, sufficient structure remains for one to be optimistic about the possibility of realizing and detecting superpositions of this sort. Reductions in the cavity loss rate  $\kappa$  and/or

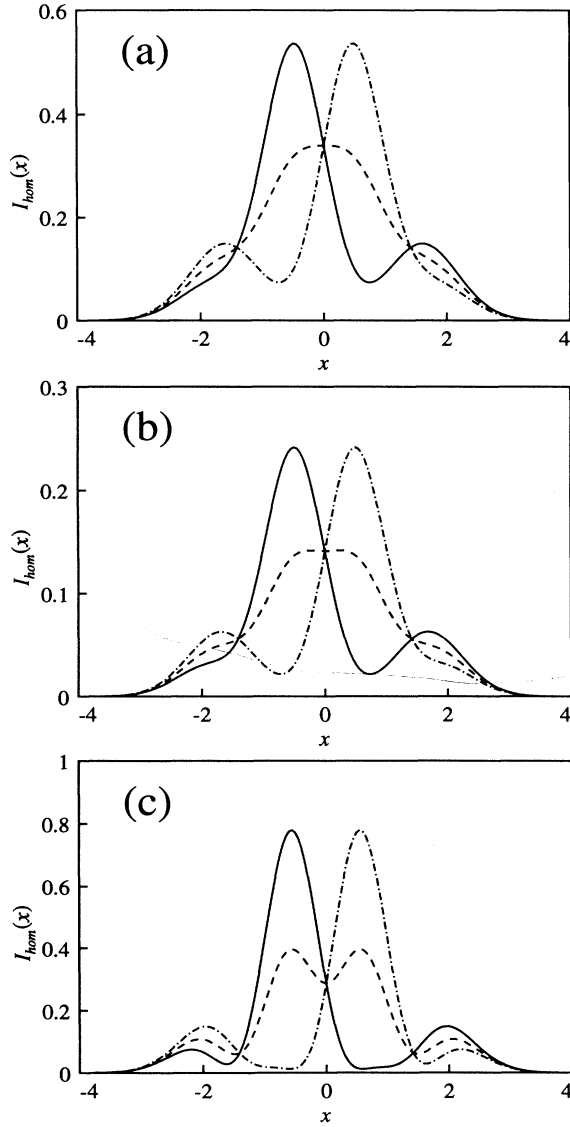


FIG. 11. Homodyne current distribution  $I_{hom}(x\theta)$  given an initial atomic state  $2^{-1/2}(|g_0\rangle + |g_{+3}\rangle)$  and parameters as in Fig. 10 ( $\kappa = 0.5$ ), with  $\theta = 0$  (solid curve),  $\pi/6$  (dashed curve), and  $\pi/3$  (dot-dashed curve). The integration interval is (a)  $(T_0, T_1) = (2, 3)$  and (b)  $(2.2, 2.6)$ . The limiting case  $\kappa \rightarrow 0$  is shown in (c).

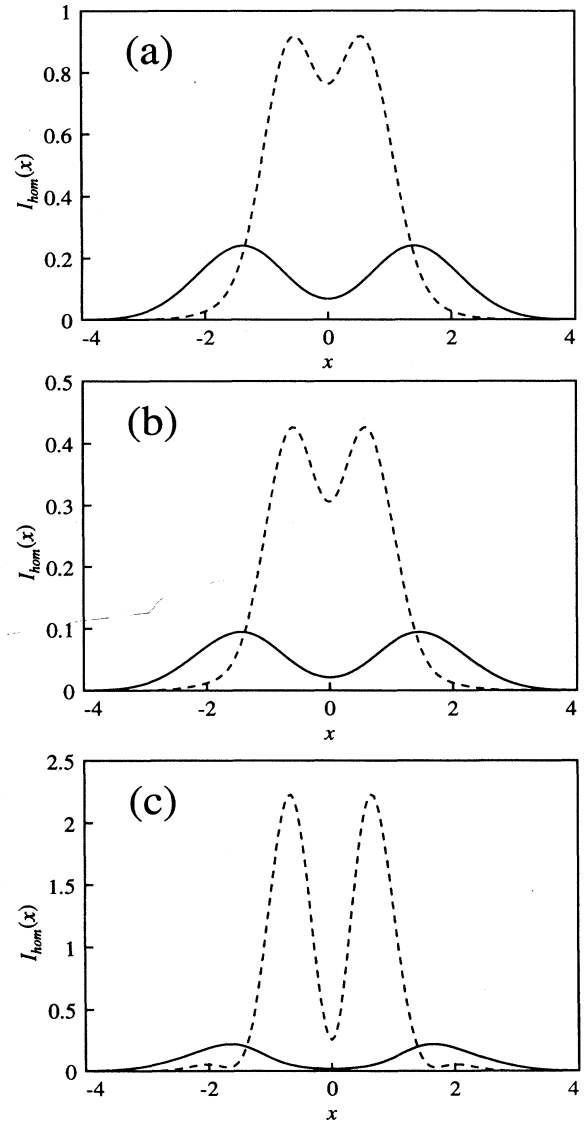


FIG. 12. Homodyne current distribution  $I_{hom}(x\theta)$  given an initial atomic state as in Eq. (26) and parameters as in Fig. 10 ( $\kappa = 0.5$ ), with  $\theta = 0$  (solid curve) and  $\pi/2$  (dashed curve). The integration interval is (a)  $(T_0, T_1) = (2, 3)$  and (b)  $(2.2, 2.6)$ . The limiting case  $\kappa \rightarrow 0$  is shown in (c).

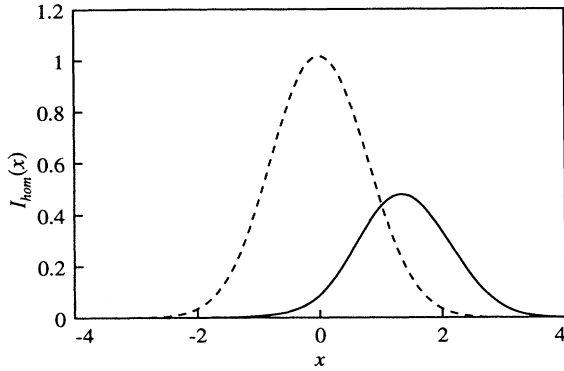


FIG. 13. Homodyne current distribution  $I_{hom}(x_\theta)$  given an initial atomic state as in Eq.(28) and parameters as in Fig. 10 ( $\kappa = 0.5$ ), with  $\theta = 0$  (solid curve) and  $\pi/2$  (dashed curve). The integration interval is  $(T_0, T_1) = (2, 3)$ .

increases in the coupling strength  $g_{max}$  naturally lead to improvements in the results presented in the figures.

For completeness, and as an additional comparison, we also give, in Fig. 13, the results obtained for an initial atomic state

$$\mathcal{N}e^{-|\alpha|^2/2} \left( |g_{+3}\rangle + \alpha|g_{+2}\rangle + \frac{\alpha^2}{\sqrt{2!}}|g_{+1}\rangle + \frac{\alpha^3}{\sqrt{3!}}|g_0\rangle + \frac{\alpha^4}{\sqrt{4!}}|g_{-1}\rangle + \frac{\alpha^5}{\sqrt{5!}}|g_{-2}\rangle + \frac{\alpha^6}{\sqrt{6!}}|g_{-3}\rangle + \frac{\alpha^7}{\sqrt{7!}}|g_{-4}\rangle \right), \quad (28)$$

corresponding to the preparation of the coherent state  $|\alpha\rangle$ . The same parameters are used as for Fig. 12(a).

### V. COHERENT SUPERPOSITIONS OF SEPARATED CAVITY FIELDS

A variation on the ideas presented above can also be used to prepare superposition states of *macroscopically separated cavity fields* [5]. Consider, for example, two separated cavity modes, each of which is overlapping with a laser field in the adiabatic passage configuration. The two cavity fields are of identical linear polarization and are coupled to the  $J_g = 1 \rightarrow J_e = 0$  transition of a single atom passing through the cavities. The laser fields in the first and second cavities are  $\sigma^+$  and  $\sigma^-$  polarized, respectively. The atom is assumed to be initially prepared in a coherent superposition of the ground states  $|g_{-1}\rangle$  and  $|g_{+1}\rangle$ . It is straightforward to show that passage of the atom through the two (consecutive) interaction zones the transformation (under ideal conditions)

$$\begin{aligned} & \frac{1}{\sqrt{2}} (|g_{-1}\rangle + |g_{+1}\rangle) \otimes |0, 0\rangle \\ & \rightarrow \frac{1}{\sqrt{2}} (|g_0\rangle \otimes |1, 0\rangle + |g_{+1}\rangle \otimes |0, 0\rangle) \quad (\text{first cavity}) \\ & \rightarrow \frac{1}{\sqrt{2}} |g_0\rangle \otimes (|1, 0\rangle + |0, 1\rangle) \quad (\text{second cavity}), \quad (29) \end{aligned}$$

where  $|a, b\rangle \equiv |a\rangle|b\rangle$  denotes the state with  $a$  photons in the first cavity and  $b$  photons in the second cavity. Hence a coherent superposition state of the fields in the two cavities is prepared, provided of course that cavity dissipation is sufficiently small.

More general superposition states of two, or even more, cavity fields can in principle be constructed by considering atomic transitions of higher Zeeman degeneracy. Multiple-photon Fock states of the individual cavity fields are also possible with such a scheme.

### VI. QUANTUM MEASUREMENT OF THE CAVITY FIELD

In our previous work [19], we briefly mentioned the possibility of measuring as well as of generating quantum states of the cavity field. The purpose of this section is to elaborate this point further with reference to a particular scheme for quantum measurement of the intracavity photon number. However, quite apart from any specific example, we wish to emphasize the reversible nature of the adiabatic passage scheme whereby complete information about the state of the intracavity field can be mapped to the Zeeman coherence of an atom. That is, if we consider a reversal of the atomic velocity shown in Fig. 1, then the mapping of Eq. (22) is likewise reversed with the coefficients  $c_m$  for the intracavity field now appearing as the probability amplitudes for the various Zeeman sublevels. Note that the intracavity field is left in the vacuum state after the atomic transit independent of the initial field state [subject only to the conditions appropriate to adiabatic transfer with low dissipation as expressed in Eq. (16) and to the constraint of a maximum photon number consistent with the atomic level scheme employed]. Hence the mapping of the wave function for the intracavity field to that of the atom as expressed by a reversal of Eq. (22) is universal in that it applies to arbitrary field states which are *a priori* unknown and as such should serve as a powerful tool within the domain of quantum measurement.

As a particular example to illustrate this general capability, we propose a scheme for quantum measurement of the intracavity photon number [36]. In qualitative terms, the notion is to employ the inverse transformation of Eq. (22) whereby photons in the cavity are first removed and “read” by an atomic transit and are then replaced back into the cavity mode by the transformation Eq. (22). More specifically, imagine an atom that transits the cavity “backwards” relative to Fig. 1 so that the photon statistics of the cavity field are transferred to Zeeman coherence of the atom for the states  $g_m$ . If the field were initially in a Fock state, then a single Zeeman state would result; otherwise, a superposition of Zeeman states would be the outcome. In the former case, an irreversible measurement of the atomic state (e.g., by state-selective photoionization or by optical-microwave double-resonance spectroscopy) would always yield a unique value for  $g_m$  and hence the original photon number. In the latter case, the measurement would (randomly) “project” the atom

into one of the several Zeeman states, with a resulting distribution  $\{g_m\}$  that reflects the original distribution for the intracavity photon number. In either case, given  $g_m$ , the procedure would be reversed to send an atom (perhaps even the original atom) through the cavity to generate the appropriate Fock state for the intracavity field. Hence, if the cavity field were originally to be in a certain Fock state, it is restored to precisely this state after the second atomic transit. If, on the other hand, the cavity field were not to be in a Fock state initially, it would nonetheless be projected by the measurement process into a final state which is a Fock state with the particular value for the intracavity photon number determined from the number distribution for the initial field state. Thus, because this first measurement sequence results in a Fock state independent of the initial field distribution, subsequent repetitions of this sequence would yield a single unique value for  $g_m$  and hence for the intracavity photon number.

Notwithstanding the intermediate steps for the above sequence (i.e., for the first “read” atomic transit, then for the vacuum field between transits, and finally for the second “restore” atomic transit), this scheme functions overall in a fashion resembling a backaction evading (BAE) measurement of the photon number of the cavity field [37]. In regard to the intermediate steps, note that a lack of the strict preservation of the state of the “signal” field is implicit in many BAE schemes, with deviations arising anytime that the signal-meter coupling is implemented by way of finite elements. For example, recent BAE measurements of the quadrature-phase amplitude of a signal beam employ first a polarization rotation followed by parametric amplification and finally completed by a second rotation of polarization [38]. The state of the incident signal field is not preserved in these various intermediate stages, but rather only by the overall transformation. Likewise in our present example, the state of the intracavity field is maintained only from the perspective of the global interaction. Here we make explicit the intermediate state for the signal field which is being measured; it is the vacuum state. In many respects the spirit of our current proposal is similar to that embodied in recent demonstrations of “quantum repeaters” for which a (broad bandwidth) field is (irreversibly) recorded by a photodetector and is then subsequently “recreated” by an emitting device with high efficiency [39], although arguably these particular schemes give only approximate measures of the field states with respect to photon flux.

Turning to a somewhat more general perspective, we note that since the complete state of the intracavity field is specified by the coefficients  $\{c_m\}$  that are transferred to the atom, our proposed measurement technique is in principle capable of a wide set of quantum measurements beyond simply that of photon number. Indeed, to the extent that superpositions of the various  $\{c_m\}$  for the Zeeman levels  $\{g_m\}$  can be recorded in the intermediate interval after the transit of the first atom (such as, for example, by an adiabatic change of the atomic basis affected by rotation in a magnetic field), a variety of measurements would be possible, including the quadrature-phase amplitude. Furthermore, within the constraints

imposed by dissipation, our scheme can be readily repeated for successive measurements of the intracavity field (in the fashion of quantum nondemolition measurement [40]).

A variation of these basic ideas for measurement via adiabatic transfer is to employ a cavity with separated “lobes” for its mode structure (such as a TEM<sub>01</sub> mode or the two arms of a ring cavity [41]). In this arrangement, the field would be read in the region of the first field lobe by the transit of an atom, this atom would then be interrogated in the intermediate region where the cavity amplitude is zero, and finally the field would be restored by transit of the atom through the second cavity lobe. Note that the measurement of the state of the atom in the intermediate region could be either “reversible” (involving, for example, a Stern-Gerlach deflection in a magnetic field gradient) or “irreversible” (involving, for example, state-selective photoionization). If a reversible technique were to be employed, then the restoration of the field state would be distinctly different from that discussed above in that the overall state of the atom-cavity system after atomic transit through the second lobe would no longer be a direct product state, but instead would in general be an entangled state. Stated more explicitly, if, for example, the measurement in the intermediate region involved a coupling of the internal Zeeman state to the external atomic center-of-mass motion, then an entangled state would be generated for the restored field state and that of the atomic momentum and hence the state of the cavity field would not be known (or indeed objectively exist) until a measurement of the atomic momentum were made, possibly long after the atomic transit through the mode.

Beyond the independent transits of individual atoms, interesting possibilities also arise from sequential atomic transits and the quantum correlations thereby produced. For example, if the measurement that collapses the entangled atom-field state is postponed, then multiple atoms which pass through the state-mapping apparatus within a sufficiently short time interval should emerge with mutually entangled states. By a suitable trace over the field degrees of freedom, it might then be possible to generate a sequence of atoms with correlated internal states, which could find application in investigations of nonlocality in quantum mechanics.

Although the analytical capabilities demonstrated in the preceding sections are certainly applicable to the discussion of quantum measurement of the cavity field presented in this section, we will postpone to a future work a thorough quantitative analysis based upon numerical solutions of the master equation and upon quantum trajectories. As for the experimental implementation of these ideas, we note that a principal requirement beyond that discussed in connection with Figs. 6–8 is the need for a much smaller dissipation rate for the cavity (without a concomitant sacrifice in coupling strength  $g$ ). The most promising route to this end would seem to be adiabatic transfer which employs the external fields of microspheres, as will be discussed in the Conclusion and for which cavity storage times sufficient for multiple atomic transits seem feasible.

## VII. CONCLUSION

In this paper we have expanded upon the work presented in Ref. [19] and taken a step towards modeling likely experimental situations and measurements. Our models required certain assumptions of considerable relevance to potential experimental configurations and here we would like to discuss some of these assumptions further.

First, the photon-counting and homodyne measurements that we presented assumed the ability to detect the passage of single atoms through the interaction region. As a potential configuration, we can suggest the following setup, which makes further use of cavity QED effects in the strong coupling limit. A dilute atomic beam passes through a preliminary cavity before entering the adiabatic passage region. Given a sufficiently strong atom-cavity-mode coupling in the preliminary cavity, passage of a single atom through this cavity produces an observable change (in real time) in the transmission of a signal through the cavity. This change serves as a trigger for the photon-counting measurement of the field in the second cavity. The extent of the modification to the transmission also provides information on the location of the atom relative to the antinodes of the standing-wave cavity field, which, given that the first and second cavities are stabilized relative to each other, can be used to select only those atoms passing through antinodes of the cavity in which adiabatic passage occurs (thus maximizing the coupling strength  $g_{max}$ ). Physical gratings might also be employed to help guide atoms through the cavity antinodes. Alternatively, the atom-detection stage could be placed after the adiabatic passage region and atom detections could be correlated with photon-counting or homodyne detection intervals.

For our study of the preparation of coherent superposition states, we assumed somewhat idealized initial superposition states of the atomic ground-state sublevels. While these particular states may not be straightforward to prepare, it is clear that a great variety of superposition states (which should exhibit similar properties to the states we considered) could be prepared in practice using, for example, radio-frequency pumping or by introducing rotations of the quantization axis between preparatory and interaction regions. In this work, we have also limited our considerations to  $J_g = 4 \rightarrow J_e = 3$  atomic transitions. Higher angular momentum states could also be considered, expanding the range of possibilities for the preparation of superposition states.

Finally, the requirement of strong atom-cavity-mode coupling relative to spontaneous emission and cavity loss rates is fundamental to the scheme. Our emphasis has been on parameter regimes that are hopefully within reach of present state-of-the-art cavity QED experiments using cesium atoms in an optical Fabry-Pérot cavity, where parameter ratios  $g_{max} : \Gamma : \kappa \simeq 7.2 : 5 : 1.2$  have been achieved [27].

An alternative and interesting prospect for experiments in cavity QED, alluded to at the end of Sec. VI, is the dielectric microsphere [42–44]. Optical (“whispering gallery”) modes circulating just inside the surface of

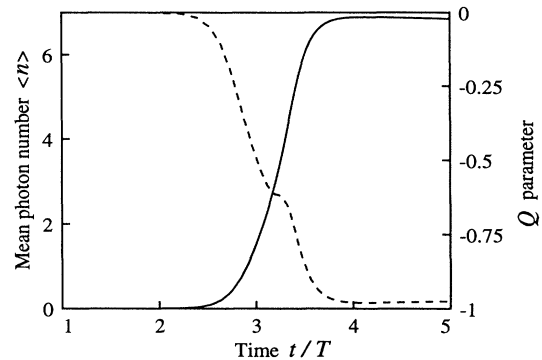


FIG. 14. Mean cavity-mode photon number  $\langle n \rangle$  (solid line) and cavity-field Mandel  $Q$  parameter (dashed line) as a function of time for parameters appropriate to a microsphere configuration (see text). An atomic  $J_g = 4 \rightarrow J_e = 3$  transition is considered with initial system state  $|g_{-4}\rangle \otimes |0\rangle$ . The parameters are  $\Gamma = 5$ ,  $g_{max} = 125$ ,  $\Omega_{max} = 150$ , and  $\kappa = 0.0035$ . The Gaussian pulses  $g(t)$  and  $\Omega(t)$  have FWHM  $T = 1$  and are centered at  $t = 2.7$  and  $t = 3.4$ , respectively. The population in the atomic state  $|g_{+3}\rangle$  following the transfer is 0.974.

the sphere possess an evanescent component external to the sphere which can interact with atoms close to the surface. These modes exhibit extremely large quality factors  $Q$  and, because of the very small electromagnetic mode volumes associated with microspheres, large atom-field coupling coefficients  $g_{max}$  can simultaneously be realized. For example, calculations presented in Ref. [44] suggest that a parameter set  $g_{max} : \Gamma : \kappa \simeq 125 : 5 : 0.0035$  could be achieved for cesium atoms brought close to the surface of a microsphere of radius  $R \simeq 9 \mu\text{m}$  and coupled to a mode of quality factor  $Q \simeq 10^{11}$ . In Fig. 14 we plot the mean photon number and  $Q$  parameter as a function of time (as in Sec. III B) for this parameter set and for a  $J_g = 4 \rightarrow J_e = 3$  atomic transition with initial atomic state  $|g_{-4}\rangle$  (i.e., we attempt to generate a seven-photon Fock state of the field). The results are seen to be close to ideal and the long lifetime of the field state makes the microsphere scheme of special relevance to the ideas presented in Secs. IV–VI for the preparation of macroscopic superposition states and for sequential measurements of cavity fields.

## ACKNOWLEDGMENTS

A.S. Parkins thanks JILA for hospitality during a stay when part of this work was carried out, and is supported at the Universität Konstanz by the Alexander von Humboldt Foundation. The work at JILA is supported in part by the NSF, while that at Caltech is supported by the NSF and the ONR.

## APPENDIX: MONTE CARLO WAVE-FUNCTION SIMULATION

The procedure we follow is that described and implemented in the papers of Dum *et al.* [31], so for more

details the reader is referred to that work. The basic approach is summarized by the following steps.

(i) For each atom, or trajectory, we begin with an initial state  $|\psi(t=0)\rangle$  describing a decoupled atom and cavity mode (for example,  $|g_k\rangle \otimes |0\rangle_{cav}$ ).

(ii) A uniform random deviate  $r \in (0, 1)$  is generated and the wave function is propagated according to

$$\frac{\partial}{\partial t} |\psi(t)\rangle = -iH_{eff}(t) |\psi(t)\rangle \quad (\text{A1})$$

[where  $H_{eff}(t)$  is given by Eq. (18)], until such time as the norm of the wave function satisfies

$$\| |\psi(t_j)\rangle \|^2 = r \quad (\text{A2})$$

[the norm of the wave function decays because the effective Hamiltonian  $H_{eff}(t)$  is non-Hermitian].

For the case of a  $J_g = 4 \rightarrow J_e = 3$  transition, as we consider in the numerical simulations presented in this paper, the explicit form for  $H_{eff}(t)$  is

$$\begin{aligned} H_{eff}(t) = & (\Delta - i\Gamma/2) \sum_{m=-3}^{+3} |e_m\rangle \langle e_m| - i\frac{\kappa}{2} a^\dagger a \\ & - i\Omega(t)(A_{+1} - A_{+1}^\dagger) + ig(t)(a^\dagger A_0 - A_0^\dagger a), \end{aligned} \quad (\text{A3})$$

with

$$\begin{aligned} A_0 = & -\sqrt{\frac{7}{36}} |g_{-3}\rangle \langle e_{-3}| - \sqrt{\frac{1}{3}} |g_{-2}\rangle \langle e_{-2}| \\ & -\sqrt{\frac{5}{12}} |g_{-1}\rangle \langle e_{-1}| - \frac{2}{3} |g_0\rangle \langle e_0| - \sqrt{\frac{5}{12}} |g_{+1}\rangle \langle e_{+1}| \\ & -\sqrt{\frac{1}{3}} |g_{+2}\rangle \langle e_{+2}| - \sqrt{\frac{7}{36}} |g_{+3}\rangle \langle e_{+3}|, \end{aligned} \quad (\text{A4})$$

$$\begin{aligned} A_{+1} = & \sqrt{\frac{7}{9}} |g_{-4}\rangle \langle e_{-3}| + \sqrt{\frac{7}{12}} |g_{-3}\rangle \langle e_{-2}| \\ & + \sqrt{\frac{5}{12}} |g_{-2}\rangle \langle e_{-1}| + \sqrt{\frac{5}{18}} |g_{-1}\rangle \langle e_0| + \sqrt{\frac{1}{6}} |g_0\rangle \langle e_{+1}| \\ & + \sqrt{\frac{1}{12}} |g_{+1}\rangle \langle e_{+2}| + \sqrt{\frac{1}{36}} |g_{+2}\rangle \langle e_{+3}|, \end{aligned} \quad (\text{A5})$$

$$\begin{aligned} A_{-1} = & \sqrt{\frac{1}{36}} |g_{-2}\rangle \langle e_{-3}| + \sqrt{\frac{1}{12}} |g_{-1}\rangle \langle e_{-2}| \\ & + \sqrt{\frac{1}{6}} |g_0\rangle \langle e_{-1}| + \sqrt{\frac{5}{18}} |g_{+1}\rangle \langle e_0| + \sqrt{\frac{5}{12}} |g_{+2}\rangle \langle e_{+1}| \\ & + \sqrt{\frac{7}{12}} |g_{+3}\rangle \langle e_{+2}| + \sqrt{\frac{7}{9}} |g_{+4}\rangle \langle e_{+3}|. \end{aligned} \quad (\text{A6})$$

(iii) At the time  $t_j$ , a wave-function collapse, or quantum jump, occurs, corresponding to either (a) a photon emission from the cavity or (b) a spontaneous emission from the atom with polarization  $\sigma = 0, \pm 1$ . The relative probabilities for these jumps are obtained from the quantities

$$\kappa \| a|\psi(t_j)\rangle \|^2, \quad \Gamma \| A_\sigma |\psi(t_j)\rangle \|^2 \quad (\sigma = 0, \pm 1). \quad (\text{A7})$$

Dividing up the interval  $(0, 1)$  according to these relative probabilities, another uniform random deviate is generated and its position on this interval selects which one of the four possible jumps occurs. The wave function is then transformed as

$$|\psi(t_j)\rangle \longrightarrow \frac{a|\psi(t_j)\rangle}{\| a|\psi(t_j)\rangle \|} \quad \text{or} \quad \frac{A_\sigma |\psi(t_j)\rangle}{\| A_\sigma |\psi(t_j)\rangle \|} \quad (\sigma = 0, \pm 1). \quad (\text{A8})$$

One then returns to step (ii) and repeats the process until the propagation has reached the desired endpoint.

The number of cavity emissions per atom is recorded and the entire procedure is repeated for many atoms so as to generate a probability distribution. The density operator for the system at a particular time  $t$  can also be obtained by averaging over many single-atom trajectories:

$$\rho(t) = \left\langle \left\langle \frac{|\psi(t)\rangle \langle \psi(t)|}{\langle \psi(t)|\psi(t)\rangle} \right\rangle \right\rangle. \quad (\text{A9})$$

We have computed  $\rho$  in this way and found good agreement with the direct numerical solution of the master equation.

We also note that the wave-function simulation technique offers the potential for a much more comprehensive analysis of the adiabatic passage configuration than is presented here. A variety of other factors influencing a realistic experiment could be straightforwardly incorporated into the calculations.

- 
- [1] J. Opt. Soc. Am. B **4** (10) (1987) special issue on squeezed states of the electromagnetic field, edited by H.J. Kimble and D.F. Walls.
- [2] J. Mod. Opt. **34** (617) (1987) special issue on squeezed light, edited by P.L. Knight and R. Loudon.
- [3] Appl. Phys. B **55** (3) (1992) special issue on quantum noise reduction in optical systems, edited by C. Fabre and E. Giacobino.
- [4] C.W. Gardiner, Phys. Rev. Lett. **56**, 1917 (1986).
- [5] For example, see the review by P. Meystre, in *Progress in Optics*, Vol. XXX, edited by E. Wolf (North-Holland, Amsterdam, 1992), Chap. V.
- [6] G. Rempe, F. Schmidt-Kaler, and H. Walther, Phys. Rev. Lett. **64**, 2783 (1990).
- [7] F. Bernardot, P. Nussenzeig, M. Brune, J.M. Raimond, and S. Haroche, Europhys. Lett. **17**, 33 (1992).
- [8] G. Rempe, R.J. Thompson, R.J. Brecha, W.D. Lee, and H.J. Kimble, Phys. Rev. Lett. **67**, 1727 (1991).
- [9] R.J. Thompson, G. Rempe, and H.J. Kimble, Phys. Rev. Lett. **68**, 1132 (1992).
- [10] J.M. Raimond *et al.*, in *Laser Spectroscopy IX*, edited by M.S. Feld, J.E. Thomas, and A. Mooradian (Academic,

- New York, 1989), p. 140.
- [11] M. Brune, S. Haroche, V. Lefevre, J.M. Raimond, and N. Zagury, *Phys. Rev. Lett.* **65**, 976 (1990).
- [12] M.J. Holland, D.F. Walls, and P. Zoller, *Phys. Rev. Lett.* **67**, 1716 (1991).
- [13] J.I. Cirac, R. Blatt, A.S. Parkins, and P. Zoller, *Phys. Rev. Lett.* **70**, 762 (1993). The emphasis in this work is in fact on the preparation of motional Fock states of a trapped ion, but the same scheme can in principle be applied to a cavity QED configuration and to the generation of photon Fock states. More recently, J.I. Cirac, R. Blatt, and P. Zoller, *Phys. Rev. A* **49**, R3174 (1994), have also proposed a scheme for the preparation of “motional” Fock states in an ion trap using the same adiabatic passage principle employed in the present paper.
- [14] M. Brune, S. Haroche, J.M. Raimond, L. Davidovich, and N. Zagury, *Phys. Rev. A* **45**, 5193 (1992).
- [15] J.J. Slosser, P. Meystre, and E.M. Wright, *Opt. Lett.* **15**, 233 (1990).
- [16] C.M. Savage, S.L. Braunstein, and D.F. Walls, *Opt. Lett.* **15**, 628 (1990).
- [17] K. Vogel, V.M. Akulin, and W.P. Schleich, *Phys. Rev. Lett.* **71**, 1816 (1993).
- [18] B.M. Garraway, B. Sherman, H. Moya-Cessa, P.L. Knight, and G. Kurizki, *Phys. Rev. A* **49**, 535 (1994).
- [19] A.S. Parkins, P. Marte, P. Zoller, and H.J. Kimble, *Phys. Rev. Lett.* **71**, 3095 (1993).
- [20] See, for example, A. Messiah, *Quantum Mechanics* (North-Holland, Amsterdam, 1962), Vol. II.
- [21] J. Oreg, F.T. Hioe, and J.H. Eberly, *Phys. Rev. A* **29**, 690 (1984).
- [22] C.E. Carroll and F.T. Hioe, *Phys. Rev. A* **42**, 1522 (1990); *J. Opt. Soc. Am. B* **5**, 1335 (1988); F.T. Hioe and C.E. Carroll, *ibid.* **37**, 3000 (1988).
- [23] J.R. Kuklinski, U. Gaubatz, F.T. Hioe, and K. Bergmann, *Phys. Rev. A* **40**, 6741 (1989).
- [24] U. Gaubatz, P. Rudecki, S. Schieman, and K. Bergmann, *J. Chem. Phys.* **92**, 5363 (1990).
- [25] P. Marte, P. Zoller, and J.L. Hall, *Phys. Rev. A* **44**, R4118 (1991); the scheme proposed by these authors has recently been implemented experimentally by J. Lawall and M. Prentiss, *Phys. Rev. Lett.* **72**, 993 (1994), and by L.S. Goldner, C. Gerz, R.J.C. Spreeuw, S.L. Rolston, C.I. Westbrook, W.D. Phillips, P. Marte, and P. Zoller, *ibid.* **72**, 997 (1994).
- [26] If we take the specific example of cesium, then frequencies are scaled in units of  $2\pi \times 10^6 \text{ s}^{-1}$ , so that  $\Gamma = 5$  corresponds to an atomic spontaneous emission rate of  $3.1 \times 10^7 \text{ s}^{-1}$ . Suitable units of time would be  $(2\pi \times 10^6)^{-1} \text{ s}$ , so that  $T = 1$  corresponds to an interaction time of 159 ns.
- [27] R.J. Thompson, O. Carnal, and H.J. Kimble (unpublished); H.J. Kimble, in *Cavity Quantum Electrodynamics, Advances in Atomic, Molecular, and Optical Physics, Supplement 2*, edited by P.R. Berman (Academic, San Diego, 1994).
- [28] See, for example, P.R. Rice and H.J. Carmichael, *IEEE J. Quantum Electron.* **24**, 1351 (1988).
- [29] H.J. Carmichael, in *An Open Systems Approach to Quantum Optics*, edited by W. Beiglböck, Lecture Notes in Physics Vol. 18 (Springer, New York, 1993).
- [30] J. Dalibard, Y. Castin, and K. Mølmer, *Phys. Rev. Lett.* **68**, 580 (1992); K. Mølmer, Y. Castin, and J. Dalibard, *J. Opt. Soc. Am. B* **10**, 524 (1993).
- [31] R. Dum, P. Zoller, and H. Ritsch, *Phys. Rev. A* **45**, 4879 (1992); R. Dum, A.S. Parkins, P. Zoller, and C.W. Gardiner, *ibid.* **46**, 4382 (1992).
- [32] P.G. Kwiat, A.M. Steinberg, R.Y. Chiao, P.H. Eberhard, and M.D. Petroff, *Phys. Rev. A* **48**, R867 (1993).
- [33] D.T. Smithey, M. Beck, M.G. Raymer, and A. Faridani, *Phys. Rev. Lett.* **70**, 1244 (1993); M. Beck, D.T. Smithey, and M.G. Raymer, *Phys. Rev. A* **48**, R890 (1993); D.T. Smithey, M. Beck, J. Cooper, and M.G. Raymer, *ibid.* **48**, 3159 (1993).
- [34] H.J. Carmichael, L. Tian, W. Ren, and P. Alsing, in *Cavity Quantum Electrodynamics, Advances in Atomic, Molecular, and Optical Physics, Supplement 2* (Ref. [27]); H.J. Carmichael, P. Kochan, and L. Tian, in *Proceedings of the International Symposium on Coherent States: Past, Present, and Future* (World Scientific, Singapore, in press). In these works, optimal results are obtained when the local oscillator photon flux is chosen to decay at the same rate as the signal photon flux, i.e., at the cavity-mode energy loss rate; such a choice should also be desirable in any practical homodyne experiment testing the present scheme.
- [35] S. Song, C.M. Caves, and B. Yurke, in *Coherence and Quantum Optics VI*, edited by J.H. Eberly, L. Mandel, and E. Wolf (Plenum, New York, 1990), p. 1107.
- [36] The discussion presented in this section is based upon research carried out in collaboration with H. Mabuchi.
- [37] For recent reviews of the status of BAE measurement, see J.F. Roch *et al.*, *Appl. Phys. B* **55**, 291 (1992) and G. Taubes, *Science* **263**, 1376 (1994), and references therein.
- [38] Z.Y. Ou, S.F. Pereira, and H.J. Kimble, *Phys. Rev. Lett.* **72**, 214 (1994).
- [39] For a recent review of “quantum repeaters,” see Y. Yamamoto, *Science* **263**, 1394 (1994), and references therein.
- [40] V.B. Braginsky, Y.I. Vorontsov, and K.S. Thorne, *Science* **209**, 547 (1990); C.M. Caves, K.S. Thorne, R.W.P. Drever, V.D. Sandberg, and M. Zimmermann, *Rev. Mod. Phys.* **52**, 341 (1980).
- [41] V.B. Braginsky and F.Ya. Khalili, *Phys. Lett. A* **186**, 15 (1994), have independently put forth an idea similar to the one described above but based upon a coherent Rabi oscillation at frequency  $g$  for a two-level atom which transits two separated “lobes” of a microwave resonator.
- [42] V.B. Braginsky, M.L. Gorodetsky, and V.S. Ilchenko, *Phys. Lett. A* **137**, 393 (1989); in *Laser Optics '93* (SPIE, Bellingham, WA, in press).
- [43] L. Collot, V. Lefèvre-Seguin, M. Brune, J.M. Raimond, and S. Haroche, *Europhys. Lett.* **23**, 327 (1993).
- [44] H. Mabuchi and H.J. Kimble, *Opt. Lett.* **19**, 749 (1994).

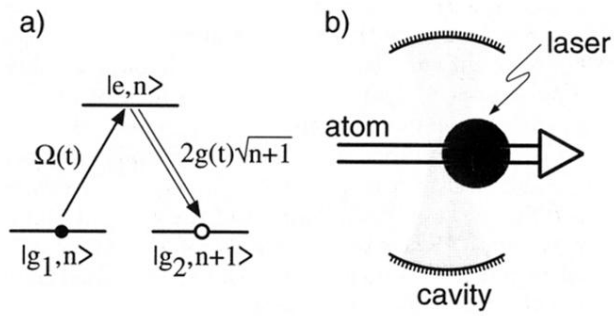


FIG. 1. (a)  $\Lambda$  three-level atom. (b) Proposed configuration for the preparation of Fock states using three-level atoms. The propagation direction of the pump laser is perpendicular to the page.